Roman Geier

pH Sensitive Responsive Gels

Masterarbeit

Zur Erlangung des akademischen Grades

Master of Science

An der Fakultät für Technische Chemie,

Verfahrenstechnik und Biotechnologie der

Technischen Universität Graz

Im Rahmen von

NAWI – Graz

Betreut durch Univ.-Prof. i. R. Dipl.-Ing. Dr. techn. Otto Glatter

Institut für Chemie

An der Karl-Franzens-Universität Graz

Deutsche Fassung:
Beschluss der Curricula-Kommission für Bachelor-, Master- und Diplomstudien vom 10.11.2008
Genehmigung des Senates am 1.12.2008

EIDESSTATTLICHE ERKLÄRUNG

Ich erkläre an Eides statt, dass ich die vorliegende Arbeit selbstständig verfasst, andere als die angegebenen Quellen/Hilfsmittel nicht benutzt, und die den benutzten Quellen wörtlich und inhaltlich entnommenen Stellen als solche kenntlich gemacht habe.

Graz, am ………………………… ……………………………………………..
(Unterschrift)

Englische Fassung:

STATUTORY DECLARATION

I declare that I have authored this thesis independently, that I have not used other than the declared sources / resources, and that I have explicitly marked all material which has been quoted either literally or by content from the used sources.

………………………… ……………………………………………..
date (signature)

Gewidmet Irmgard Geier für das Streben nach Bildung

Danksagung

Allen voran möchte ich meinem Betreuer Prof. Otto Glatter danken, der mich geduldig während der Masterarbeit begleitet hat und nie müde wurde, Dinge die im erstem Moment unverständlich waren, zu erklären und es immer geschafft hat, seine Mitarbeiter_innen auf's Neue zu motivieren und für Neues zu begeistern.

Ein ganz besonderer Dank gilt der gesamten Arbeitsgruppe Streumethoden. Dr. Angela Chemelli, die mir immer mit Rat und Tat zur Seite gestanden ist, gebührt Anerkennung. Ebenso Mag. Manuela Maurer und Franz Pirolt, welche mich fachlich als auch moralisch unterstützten.

Abseits der Universität gilt ein großer Dank meinen Eltern, welche mir es ermöglichten, mich auf das Studium zu konzentrieren. Ich danke euch für eure Begleitung über all die Jahre mit all den Höhen und Tiefen.

Meine lieben Freunde darf ich natürlich auch nicht vergessen, die mir ein wunderbares Leben auch abseits des Studiums ermöglichten. Meinen Freunden der Syracuse Runde danke ich für viele großartige Erlebnisse und für eine gewachsene Freundschaft.

Besonderer Dank gilt Josef Ehgartner. Es kann kaum einen geduldigeren Freund geben, der all meine Launen, Euphorien und sonstige Gemütszustände oft als erster und ungefiltert abbekommen hat. Ich bin sehr froh dich zu kennen und einige der prägendsten Ereignisse meines Lebens mit dir zu teilen.

Content

1.a. Zusammenfassung

Die vorliegende Masterarbeit beschäftigt sich mit sich selbst strukturierenden Gelen und Dispersionen. Je nach Zusammensetzung von Amphiphil, Öl und Wasser können verschiedene Nanostrukturen erhalten werden. Zusätzliche Parameter sind der Elektrolytgehalt, die Temperatur und der pH-Wert.

Im Folgenden werden die Einflüsse dieser Parameter diskutiert und die die Auswirkungen auf das vorliegende System methodisch untersucht. Das Phasensystem beruht auf Mischungen aus Dimodan U/J®, ein technisches Monoglyzerid, Tetradekan beziehungsweise Ölsäure für den Ölanteil und Wasser. Weitere Additive sind der Polyglycerolester PGE, Dimtehylsulfoxid, Glutamin, NaCl sowie verschiedene Farbstoffe.

Amphiphile ordnen sich je nach Zusammensetzung in diversen flüssigkristallinen Strukturen an. Die Eigenschaften dieser Phasen hängen sehr stark von der ausgebildeten Struktur ab und werden seit längerem als mögliche Medikamententransportsysteme betrachtet. Zu diesem Zweck wurden mit Farbstoff beladene Strukturen hergestellt, welche abgeschlossene Wasserkompartimente, wie zum Beispiel die inverse hexagonale Phase, oder auch Strukturen mit kontinuierlichen Wasserkänalen enthielten. Es wurde die Diffusion aus diesen Strukturen beobachtet und es wurde nach Stellschrauben gesucht um die Strukturen ineinander überzuführen.

Das Phasenverhalten wurde auch in ungesättigten Wasser Systemen untersucht um diese besser zu verstehen. Die ungesättigten Systeme sind hierbei rein von akademischem Interesse, da mögliche Applikationen mit Wasser im Überschuss einhergehen.

Das Hauptaugenmerk wurde hierbei auf die pH Abhängigkeit der Ölsäure gelegt. Diese liegt je nach pH-Wert in protonierter oder deprotonierter Form vor. Der unterschiedliche Protonierungszustand bedingt ein völlig anderes verhalten. Protonierte Ölsäure ist stark hydrophob und lagert sich daher zwischen den lipophilen Schwänzen des Amphiphils ein. Durch eine Erhöhung des pH-Wertes wird die Säuregruppe deprotoniert und die Verbindung hydrophilisiert. Durch die Deprotonierung der Säuregruppe ist diese negativ geladen. Die negativen Ladungen stoßen sich gegenseitig ab, was zu einer Vergrößerung der effektiven Kopf-

gruppengröße führt und bedingt eine Veränderung der Krümmung, welche die Strukturen beschreibt.

Es ist das Ziel Zusammensetzungen zu finden welche von diskontinuierlichen inversen hexagonalen Phasen ausgehen und durch die Variation des pH-Wertes in bikontinuierliche kubische Phasen überführt werden können. In Anbetracht des natürlichen pH-Gradienten stellt dies eine ideale Möglichkeit dar Pharmazeutika gezielt in den verschiedenen Bereichen des Verdauungstraktes frei zu setzen.

1.b. Summary

This master thesis focuses on self-assembled bulk phases and dispersions. In dependence of the surfactant, oil and water composition different nanostructures can be achieved. Those structures can be tuned by other additives and by parameters such as salinity, temperature and pH conditions.

The influences of the tuning parameters on the system used were methodically studied within this work. The phase system was based on Dimodan U/J®, a technical monoglyceride, tetradecane, or oleic acid, for the oil phase and water. Further the polyglycerol ester PGE, dimethyl sulfoxide DMSO, glutamine, NaCl and different dyes were used as additives.

Depending on the composition, amphiphilic systems assemble in different liquid crystalline structures. The properties of these phases are mainly based on the structures. Amphiphilic systems have been discussed as possible drug delivering systems for a quite long time as they can host lipophilic as well as hydrophilic compounds. We studied the different structural behaviour on dyed bulk phases. Therefore samples with enclosed water compartments and with continuous channels were produced to observe the release. Further we were looking for parameters to transfer the different structures into another.

The phase behaviour of water unsaturated systems were studied by academic interest only, as possible applications will require water saturated systems.

The main focus was put on the pH depending behaviour of oleic acid. Protonated and deprotonated oleic acid shows different behaviours. Protonated oleic acid is hydrophobic and therefore assembles around the hydrocarbon chains of the surfactant. Through the increase of the pH oleic acid deprotonates and becomes a charged amphiphile. It regroups in the interfacial area and through the charge repulsion, the effective head group increases and therefore the curvature and the structure changes.

The aim of this work is to find stable compositions, which transform from the inverse hexagonal structure to a continuous cubic, by pH variation. These phases would be ideal drug delivering systems as they can use the natural pH-gradient within the digestive tract and pharmaceutical compounds could be specifically released within the intestine.

2. Introduction

2.1. Motivation

Self-assembled liquid crystals are promising drug delivery systems, as they can host hydrophilic, amphiphilic and hydrophobic compounds. Pharmaceutically active compounds would be protected from the acidic conditions within the stomach by the surrounding lipids. The liquid crystals can form different structures through parameters like temperature, composition, ionic strength and pH-value. Those structures are well studied and phase transitions through varying water contents or temperature have been described. [1] [2] [3] [4]

The main aim of this work was to find a lipid based liquid crystal in form of a bulk phase or a nanostructured dispersion that is suitable as a carrier for hydrophilic compounds. As the behaviour of the liquid crystal is depending of the nanostructure, we were looking for a way to influence it. Temperature variation and a post preparation addition of chemicals fail as the application within the human body sets a constant temperature and for example the specific addition of oil to the liquid crystal is more than unlikely. The pH-value is therefore the most promising parameter.

The next chapters describe the systematical quest for pH sensitive compositions, which change their structure from the hexagonal H_2 to a bicontinuous cubic Pn3m, Im3m or Ia3d and the tune of parameters for water compartment size, temperature stability and preparation conditions.

2.2. Self-assembly of surfactants

Surface active agents, or short surfactants, are amphiphiles as they have functional regions. They consist out of a hydrophilic head group and a lipophilic tail. The head groups are usually made out of polar or even ionic functional groups, while the lipophilic tails is usually built of hydrocarbon chains with a minimum of eight carbon atoms. As surfactants are containing a polar and a nonpolar region they are soluble at low concentrations as single molecules in polar and nonpolar solvents, whereas they are hardly soluble in very polar or nonpolar solvents.

Surfactants will be in solution as single molecules as long as the critical micellar concentration (cmc) is undershot. If the concentration is above the cmc the molecules gather together and form nanophases. Depending on the polarity of the solvent they form micelles or inverse micelles. In water for example the hydrocarbon chains assemble in the inside and are shielded from the surrounding water by the polar head groups. The mobility of the chains within the micelles is similar as in bulk. [5] [6]

The free energy of the system is reduced by self-assembly; therefore external energy input will only accelerate the process.

Cosurfactants are molecules which are not amphiphilic enough for self-assembly but do interact with the surfactant film. Longer chained alcohols could be mentioned as examples.

2.2.1. Liquid crystals

At higher concentrations surfactants form liquid crystalline phases or mesophases, as they could be described as an intermediate state between liquid and solid. The structures of mesophases are described like solid crystals by the Bravais lattices.

There are different kinds of liquid crystals for example lyotropics, which depend on the solvent and thermotropics that are influenced by the temperature. Further liquid crystals have, according to their structure, different optical properties. Cubic phases are isotropic, whereas lamellar and hexagonal phases are anisotropic. [7] [8] [9] This optical behaviour makes it possible to characterise liquid crystals with crossed polarisation microscopy.

2.2.2. Micelles

As mentioned above micelles are formed in solution if the surfactant concentration is above the cmc and the Krafft temperature. The crystal lattice energy determines the solubility below the Krafft temperature, T_K and above the surfactants solubility increases.

The formation of micelles is thermodynamically favourable. The properties of the micelles like size and shape are depending on the surfactants, the temperature and for ionic surfactants on the ion concentration. [5] [6] [10]

2.2.3. Nanostructured dispersions

Beside bulk phases we also had a close look on the preparation and characterisation of nanostructured dispersions. Those dispersions can be obtained from hydrophobic surfactants, which self-assembly to liquid crystals in excess water. [11] [12] [13] The unsaturated glycerol monooleate system is well-known and forms bicontinuous cubic structures with excess water. Like other similar systems it transfers from the cubic to a reverse hexagonal phase through heating. A further temperature increase is leading to the inverse micellar phase that develops around 90°C. [4] As discussed later on in the experimental section we did not observe the change to the inverse micellar phase as the result of an increased temperature as our temperature studies were limited to a maximum temperature of 70°C.

To obtain dispersion of the above mentioned structures stabilisers are required. Those stabilisers are usually hydrophilic surfactants with a high molecular weight or even silica nanoparticles that form Pickering emulsions. [13] [14]

The temperature is not only influencing the structure but also the dispersion process, as the different structures have diverse physical properties. [15] [16]

2.2.4. Structure parameters

It was already mentioned that surfactants in solution can form micelles but also that other structures can be obtained as introduced in the liquid crystal paragraph. The question why a specific surfactant composition is leading to a corresponding structure could be explained by two models. There is the critical packing parameter (CPP), which summarises the parameters

of the surfactants such as the hydrophobic volume (v), the chain length (l_c) and the effective area of the hydrophilic head group (a_0). [17] [18] The CPP is described as the hydrophobic volume against the product of the chain length and head group size.

$$CPP = \frac{v}{l_c a_0} \qquad (1)$$

Approximations for the chain length and hydrophobic volumes can be done, as the physical properties of hydrocarbon chains are widely independent from outside influences, whereas this is not the case for the effective head group area.

The volume of the hydrocarbon chain could be assumed as:

$$v = 0.027(n_C + n_{Me}) \qquad (2)$$

and the length as

$$l_c = 0.15 + 0.127 n_C \qquad (3)$$

Where n_C is the number of carbons and n_{Me} the number of methyl groups. The volume is obtained in nm³ and the length in nm.

Effective head group areas are heavily influenced by the surrounding, as it depends on temperature and surfactant concentration. An increased temperature for example reduces for hydrophilic head groups the hydration that result in a smaller effective head group and therefore a lower CPP. Ionic surfactants are additionally depending on ionic strength. The effective head group area is decreasing if the salinity is increased as the counter ions shield the charged surfactants. The salt is minimizing the repulsive effect of the charged surfactants. [19]

The CPP is furthermore influenced by the pH as this changes the protonation of the head group and therefore the ionic behaviour; this is the case for functional groups which behave acidic or basic. Beside head group active parameters there are also variable properties of the lipophilic tail. Double chains or branched chains are more space demanding and therefore leading to lower CPPs. Also the grade of unsaturation of the hydrocarbon chain is influencing the structure; nevertheless these are parameters that can be set through the preparation and cannot be varied with physical parameters. [20]

The structure of the aggregates can be calculated according to the CPP. Figure 1 plots several obtained geometries from monoglycerides/ oil dispersions at various CPP-values. [21]
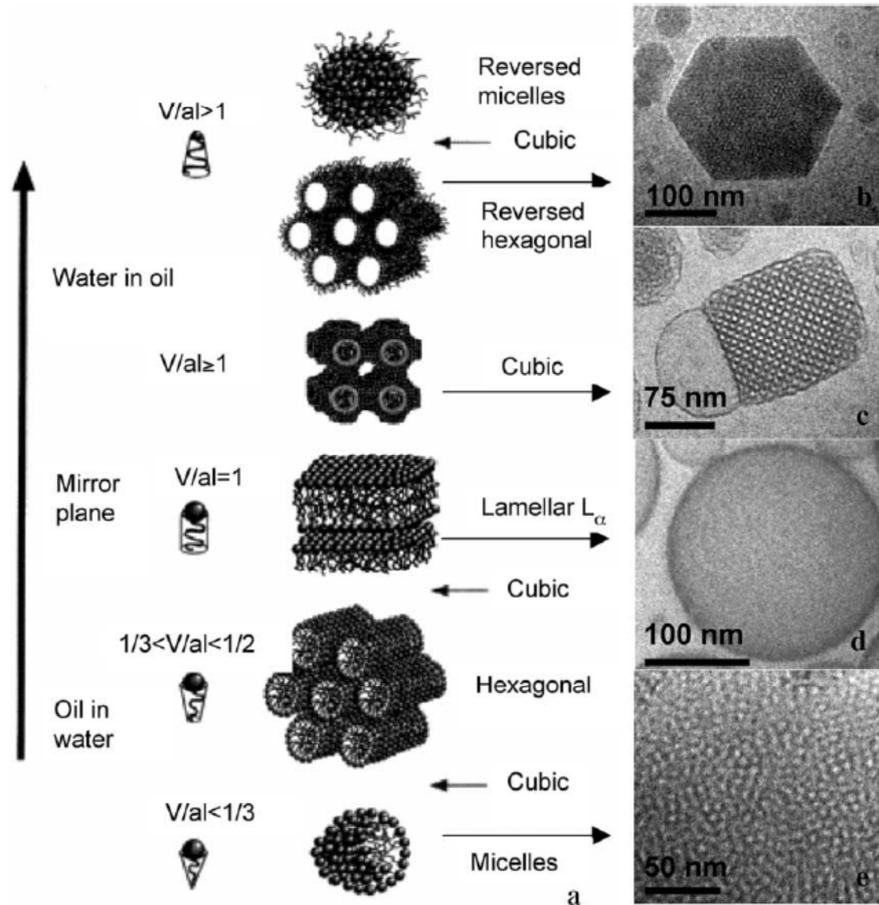
Figure 1: **Structures as a function of the CPP** with an inversion of the oil in water phase to a water in oil phase. The **cry-TEM pictures** show in b) **hexasomes**, in c) **cubosomes**, in d) **vesicles** in dispersed system at CPP=1 and in e) **normal micelles**. Figure taken from reference. [21]

The second approach to characterise self-assembled structures is to describe the hydrophilic -hydrophobic interface. A spontaneous curvature occurs in order to minimise the systems energy. The curvature is a measure for the structure and is defined as

$$c = \frac{1}{R} \qquad (4)$$

where R is the curvature radius and c the corresponding curvature.

The curvature of a surface is given as the mean curvature H.

$$H = \frac{1}{2}\left(\frac{1}{R_1} + \frac{1}{R_2}\right) \qquad (5)$$

Depending on the structure different curvatures are obtained. Spherical micelles for example have a curvature of *1/R* as R_1 and R_2 are equal. Cylinders have a mean curvature of *1/2R* as the second curvatures turns to 0 as the radius becomes infinite. Bilayers have a curvature of zero as both radii become infinite. Other structures with a mean curvature of zero could be obtained. This is the case for geometries where curvature $c_1=-c_2$ or in other words a structure that is concave and convex in the same time. Bicontinuous cubic structures show this behaviour. An additional calculated curvature, the Gaussian curvature *K*, allows us to distinguish between the cubic structures and planar bilayers. [22]
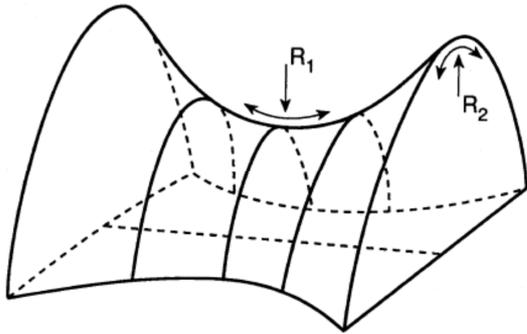
Figure 2: Schematic drawing of **a surface with zero mean curvature** in every point. Taken from reference. [10]

$$K = \left(\frac{1}{R_1} x \frac{1}{R_2}\right) \qquad (6)$$

The algebraic sign of the mean curvature is by convention positive for surfaces which bent towards the oil phase and negative for surfaces bent toward the water phase, those are the inverse mesophases.

2.2.5. Structure determination

Surfactants can form, depending on their composition and the physical parameters, different structures. Optical methods are one way of determining the structures. Small angle X-ray scattering (SAXS) is presenting an ideal method determine the structures of liquid crystalline phases, as the obtained reflections can be described by a set of lattice planes and as the lattice constants are in the range of nm.. [23] The reflections themselves correspond to specific structures according to the reflection laws. An overview, of different observed phases and there reflection laws, is given in Table 1. [24]

The distances of the planes, which describes the size of the unit cell is depending for example on the amount of water that is build into the structure, as a swelling of the water compartemnts leads to increased distances, is caluclated from the Miller indices (*hkl*). Also the type and the amount of oil in the system is influencing the lattice constants.

As additives influence the geometry this is also visible by the lattice constant. Swelling of the structures through increasing water inclusion leads within the same structure to longer parameters.

L$_\alpha$	$\left(\dfrac{a}{d}\right) = 1,2,3,4,5,6\dots$ $\quad$ with $d = \dfrac{2\pi}{q}$ and lattice parameter a
Pn3m (C$_D$)	$\left(\dfrac{a}{d_{hkl}}\right)^2 = 2,3,4,6,8,9,10,11\dots$
Ia3d (C$_G$)	$\left(\dfrac{a}{d_{hkl}}\right)^2 = 6,8,14,16,20,22,24\dots$
Im3m (C$_P$)	$\left(\dfrac{a}{d_{hkl}}\right)^2 = 2,4,6,8,10,12,14\dots$
Pm3m	$\left(\dfrac{a}{d_{hkl}}\right)^2 = 2,4,5,6,8\dots$
Fd3m	$\left(\dfrac{a}{d_{hkl}}\right)^2 = 3,8,11,12,16,19,24$
H$_2$	$\left(\dfrac{\sqrt{3}a}{2d_{hk}}\right)^2 = 1,3,4,7$

Table 1: **Reflection laws** of lamellar cubic and hexagonal space groups. d is describing the distance between the lattice planes. Adopted from reference [24]

Mixed phases are often occurring near phase boundaries and the structure determination could cause troubles. Angelov et.al. studied a similar system as we did. They investigated the phase transition of bicontinuous inverted cubic phases to inverted hexagonal phases by temperature variations and by mixing of the prepared phases. Pure glycerol monoole-ate/water systems were used as reference points and for temperature studies. To induce the bicontinuous cubic sponge phase (L$_3$) DGMO and oleic acid were added. Through measure-ments of the pure phases and fittings of specified mixtures they were able to create model fits determining coexisting sponges in with cubic phases. [25]

2.3. Phase Diagrams

Commonly surfactant systems are characterized either as binary or ternary systems, where binary systems represent the simplest compositions. They usually consist out of the surfactant and water. On the other hand ternary systems include usually oil. This means that there is another adjustable parameter. Systems of a higher order are produced but not in respect of a full phase diagram with more than 3 parameters. A ternary phase diagram in dependence of the temperature results in a phase prism based on the Gibbs triangle *ABC*. [26] Ternary or higher systems are often represented by pseudo binary phase diagrams; those are achieved by cuts through the Gibbs prism.
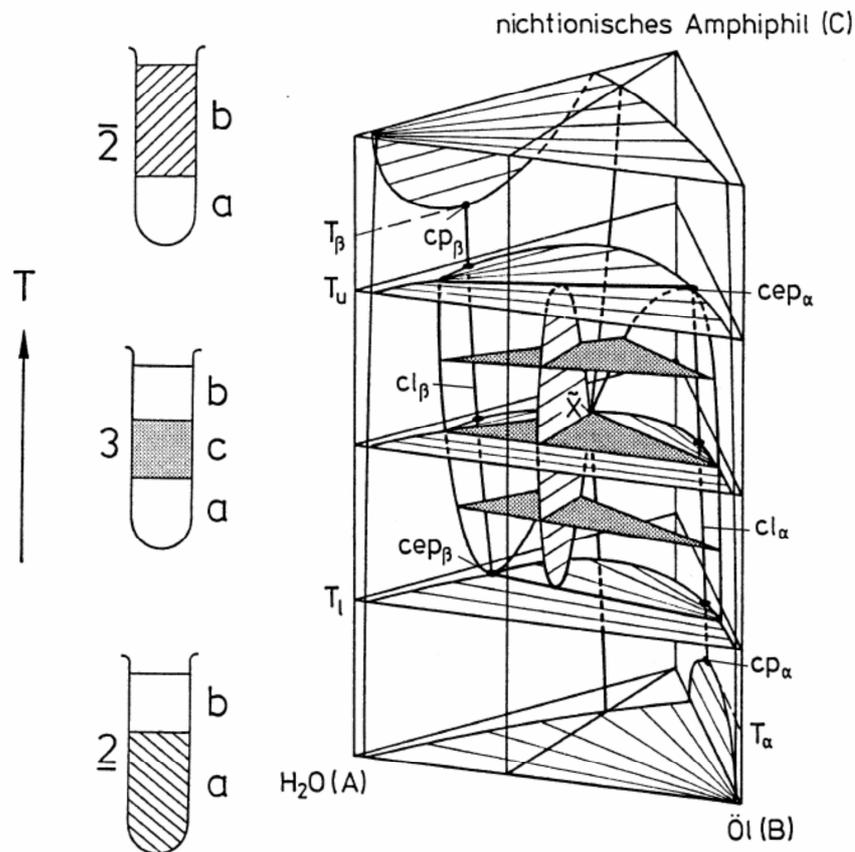
Figure 3: **Gibbs prism** based on **a ternary amphiphile**, water and oil system in dependence of the **temperature**. Figure taken from reference. [10]

Pseudo binary and binary phase diagrams plot in a clear way the phase behaviour and are expressed by the δ-value if oil is added.

$$\delta = \frac{mass\ of\ glyceride}{mass\ of\ glyceride\ +mass\ of\ oil}100 \qquad (7)$$

In this work we focus on monoglyceride based systems which are well studied. Figure 4 shows the temperature dependent phase diagram of the binary mono linolein/water system, which is similar to our Dimodan U/J®/water system. [4] [27] Dimodan U/J® consists out of 96% of distilled monoglycerides from refined sunflower, raps seed and palm oil, where the main compound is mono linolein.
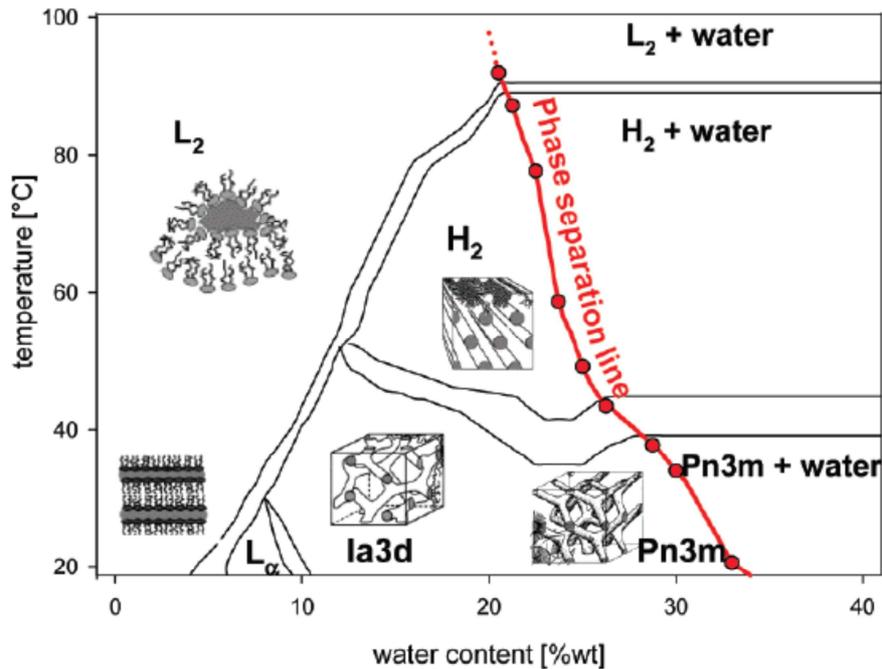
Figure 4: **Dimodan U/J® and water** system in **dependence of the temperature**. The red line represents the **phase separation**. Phases above this line are water saturated and surrounded by excess water. Parallel lines indicate mixed structures. The diagram is taken from reference [4] and was confirmed by [27]

This system develops the bicontinuous cubic phases Ia3d and Pn3m as well as the hexagonal H_2. The phase diagram shows that there is a structural transition from cubic to hexagonal when temperature is increased. By geometrical reasons the H_2 is suspected to have enclosed water compartments in contrast to the bicontinuous cubic phases. The diffusion between different water compartments of the hexagonal phase was studied and the results indicate that the compartments are connected. [28] Release studies showed that the inverse hexagonal phase is retaining hydrophilic molecules better than the bicontinuous cubic phases. [29] [30]

The idea is to start at a phase that retains molecules better and transfer it to a phase where a fast release is possible. This seems to be possible for transitions from the hexagonal to the bicontinuous cubic phase. For biological applications it is obvious that the temperature is not

an ideal parameter to initiate the structural change. Nevertheless this phase diagram shows already important facts for our purposes.

Further the Pn3m which is formed at lower temperatures incorporates more water than the H_2. The structural change is also observed in excess water. In the section about the CPP we already discussed the influence of temperature. If we start at the hexagonal phase we have a high temperature and therefore a low head group hydration, which means that the effective head group area is small and the corresponding negative mean curvature high. The cubic structure requires a lower curvature close to zero that is achieved by the increase of the effective head group area through the decrease of the temperature.

A possible responsive phase contains a head group that is changing the effective area. Long chained carbon acids are promising candidates for this purpose. As long chained carbon ac-
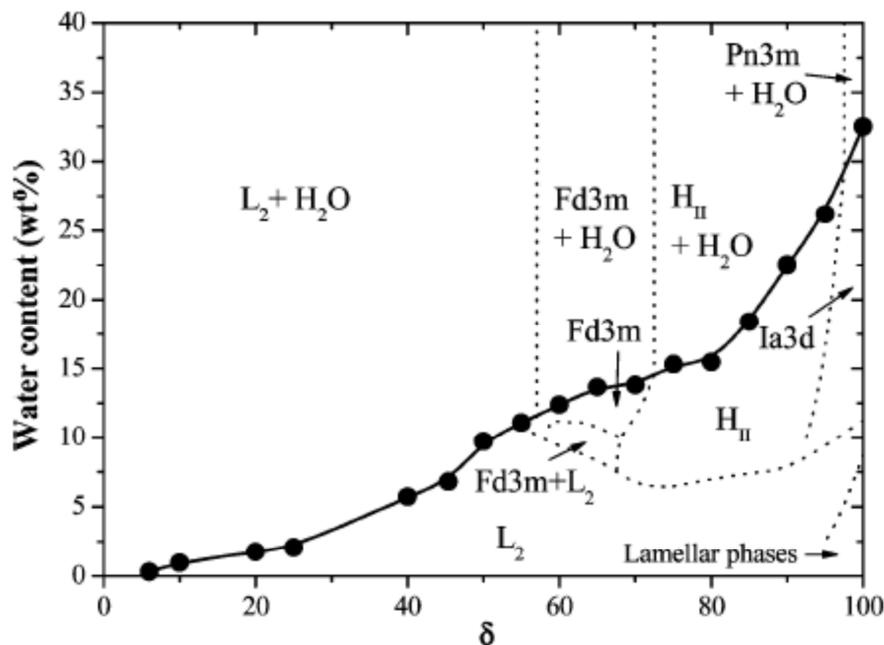
Figure 5: **Phase diagram** of **Dimodan U/J** with **R-(+)-limonene** and **water** at **25°C**. The bold line represents the phase separation. Cubic and hexagonal structures share phase boarders. [16]

ids such as oleic acid [31] have similar properties to the corresponding hydrocarbon it is appropriate to have a look on oil containing ternary systems. A well-known system of this kind is based on Dimodan U/J®, which is a technical grade monoglyceride linolein and R-(+)-limonene. [16] Systems with tetradecane are also widely used and show similar properties, within this thesis tetradecane was used as a model compound. [32] [33]

The binary phase diagram showed us that the cubic phases can be transformed to the hexagonal by temperature increase. Also the hexagonal phase can be achieved by the addition of oil as the plot above indicates. Depending on the mobility of the amphiphiles the equilibration of system may require weeks. Those mesophases are usually consisting of amphiphiles with long unsaturated hydrocarbon chains. [34] The incorporation of additives occurs in dependence of the amphiphile lateral mobility and orientation that could be observed by voltamometric techniques in case of ionic amphiphiles. [35]

The oil is implemented in the structure by coordinating with the hydrophobic chains and leads therefore to higher curvatures. Figure 6 gives a schematic representation of oil integrated oil. [29] [36]
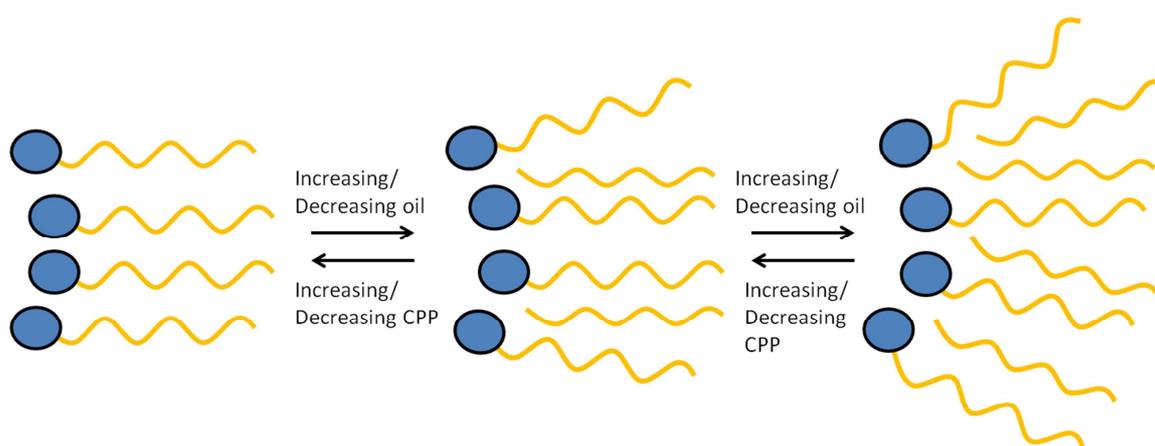
Figure 6: Schematic drawing of **oil implementation** to **surfactants** and resulting **changes in CPP**. Adopted after [29] [36]

The added oil interacts with the hydrophobic surfactant tail and therefore pushes the chains aside resulting in higher negative curvatures. This behaviour can be followed by structure determination with SAXS and for minor oil changes by the lattice parameters. An increase of the oil reduces the lattice constant. [37]

The for this work most important realisation out of the phase diagram by Salonen [16] is that both desired phases share phase borders. This means that a direct transition from hexagonal to cubic is possible without an intermediate structure. Also a swelling of the structures through water addition was observed. We decided to set up our experiments at δ-values around δ90 as this is still hexagonal but close to the cubic phase and we are also able to study the system at different water contents but with similar expected results. We will com-

pare the behaviour of our system in the water unsaturated and the saturated phase in the experimental section.

Another approach to distinguish the effect of water was described by Yeh et.al. [38] They combined the statistical association fluid theory (SAFT) with a density functional theory (DFT) and studied density fluctuations of ternary amphiphile, water and oil systems. Interfacial density variations were observed as a function of the water saturation degree.

Within our studies we went to even more complex systems with additional compounds. Polyglycerol esters influence the phase behaviour in several ways. Bilayer-based structures are stabilised by DGMO (Diglycerol monooleate) as it prefers a low curvature through the CPP. This was already reported by [39] and later in-house confirmed. [40]

A whole phase diagram of the pseudo binary Dimodan U/J®, PGE, tetradecane and water was just recently produced by Maurer. [41]
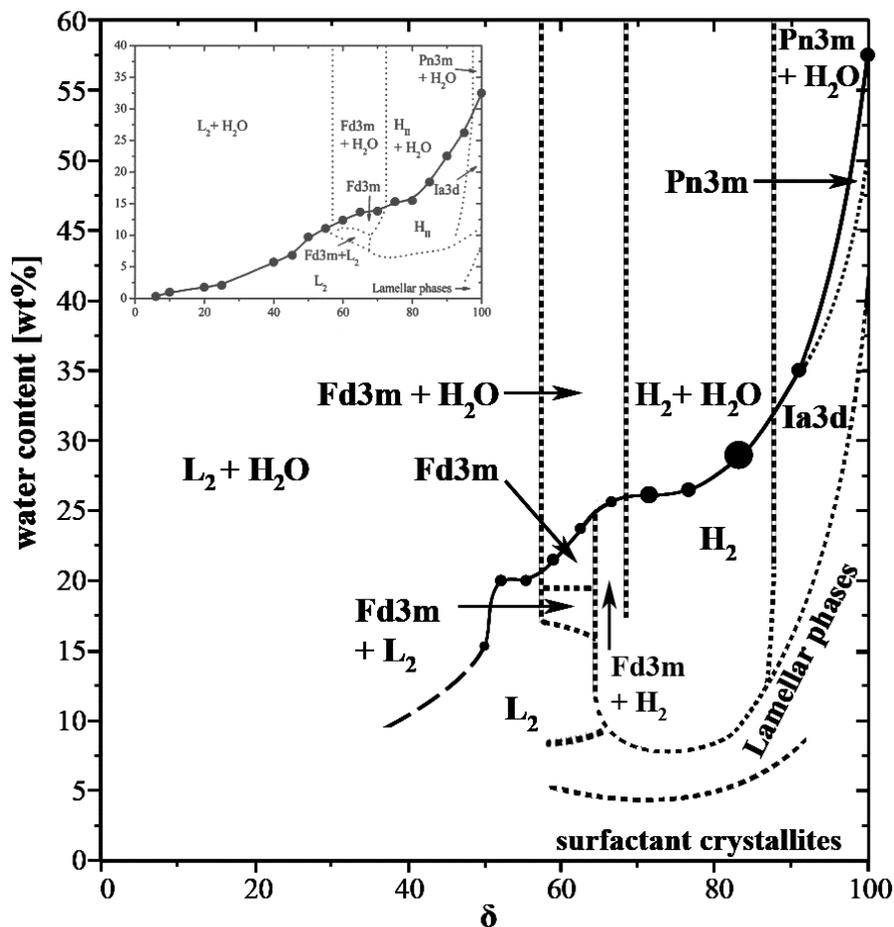
Figure 7: **Pseudo binary phase diagram** of the Dimodan U/J®, **PGE**, Tetradecane and water system **in comparison with the PGE free phase diagram** (inset). The PGE content was fixed at 33wt% of the amphiphile. The phase diagram is a function of water at 25°C. With kind permission from Maurer. [41]

The cubic and lamellar phases are both obtained over a wider area if the system is containing PGE. In particular the cubic Pn3m and Ia3d are both achieved with PGE at lower δ-values. While in the PGE free system δ90 develops still the hexagonal phase, the system with 33wt% is already cubic, either Ia3d or Pn3m, depending on the water content.

Maurer reports that those phases have a high viscosity and therefore she expects that the phase equilibration especially in temperature depending phase diagrams, needs longer than the provided time of 48 hours. [41]

Furthermore PGE containing systems are able to incorporate higher amounts of water. For δ90 about 40wt% of water can be integrated in the structure. A higher water content within
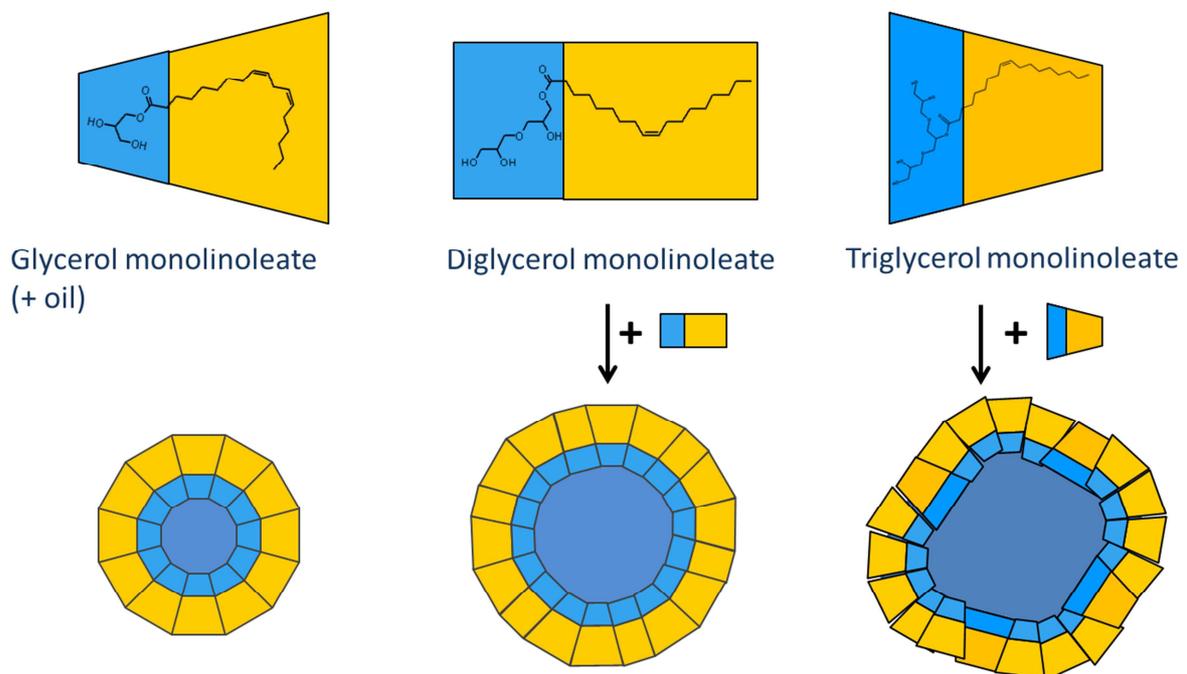
Figure 8: Schematic drawing of the **water compartment enlargement with DGMO** and induced schematic **structural change** by the usage of higher **polyglycerol esters** like Triglycerol monolinoleate. Adopted figure with kind permission from Chemelli. [29]

the phases was also achieved by using DGMO. Chemelli used DGMO to enlarge the water compartments. The DGMO was introduced to optimise the loading of the water phase with bulky additives. [29] [40] Through the increased water compartments we can assume that a diffusion of water soluble compounds or the pH equilibration would be faster in this case.

Tri and higher polyglycerides, which are part of PGE, have bigger effective head group areas compared to the diglyceride, therefore they have an even higher impact on the structure

and are pushing stronger to the cubic phases as we can recognise from Figure 8. Also we can assume larger water compartments, which effect the diffusion and equilibration.

If big head groups push towards the cubic phase, small one should prefer the hexagonal. The comparative study by Abe opposes the effect of glycerol and dimethyl-sulfoxide (DMSO) in monoolein phases. [42] The lattice parameter as a function of glycerol or DMSO concentration shows clear differences, as the lattice constants for DMSO go up and the ones for glycerol decrease. This was not verified by us and de Campo. [43]

The phase diagrams of DMSO concentration against temperature favours a mixed Pn3m and Im3m phase, while glycerol pushes towards the sole Pn3m and reduces the appearance of the mixed phase. The explanation for this behaviour is given by the Hoffmeister effect in terms of the so-called "preferential hydration phenomena. [44] DMSO behaves as a kosmotrope [45] and therefore prefers the less compact Im3m. Chaotropic salts on the other hand stabilise bicontinuous cubic phases based on hydrated monoglycerides and glycerol can be described as a chaotrope. [42] [46]

Engelskirchen et.al. showed that the addition of glycerol to phytantriol based hexasomes acts like a temperature increase, this is according to the chaotropic effects of glycerol that are mentioned above. [47]

Another possibility to influence the interface in accordance with the Hoffmeister series is the usage of zwitterions. Those ions form depending on the concentration dimers, which are hold together by H-bond assisted ion pairs. [48] Dipole-dipole and hydrophobic interactions determine the behaviour of these compounds, when they interact with surfactants. The interrelation is defined by the surfactants molar ratio and the zwitterions. [49] It is also reported that zwitterions stabilise silica particles. [50]

Amino acids are easy accessible zwitterions and were used for our studies.

2.3.1. pH influence on oleic acid containing systems

The previous descriptions stated possible parameters for tuning the structures. The intention is the creation of an ideal system that is based on the already described effects but utilises the structural change through pH variation.

As oleic acid is a carbonic acid its properties depend on the surrounding pH. The acidic behaviour is the reason why oleic acid can appear in two different protonation states. At pH-values below 7, oleic acid appears mainly in its protonated form where the lipophilic behaviour overweighs and is hardly soluble in water. Through the increase of the pH the weak acid gets deprotonated, the charge on the head group leads to an increased hydrophilicity. At pH-values above 7, oleic acid becomes an amphiphile through its polar head group and the unpolar fatty chain. Lamellar phases are found and at higher pH-values micelles can be observed. [51]

The pK_a as a measure for the acidity of carbonic acids and especially for oleic acid in water it is around 5. [52] But the pK_a is strongly depending on the system. When the deprotonated oleic acid is part of the interfacial layer, the negative charges require protons to minimise the electrostatic repulsion. This results in an increased pK_a as the protons are attached to the interface and not complete free. [51] To reduce this effect salt can be added.

pK_a-values between 6 and 7 were determined in monoglyceride monoolein dispersions with oleic acid under different pH conditions and various amounts of containing oleic acid. [36] [53] The structural change through the pH variation enabled the identification of the pK_a. Small additions of base close to the pK_a resulted in huge structural changes.
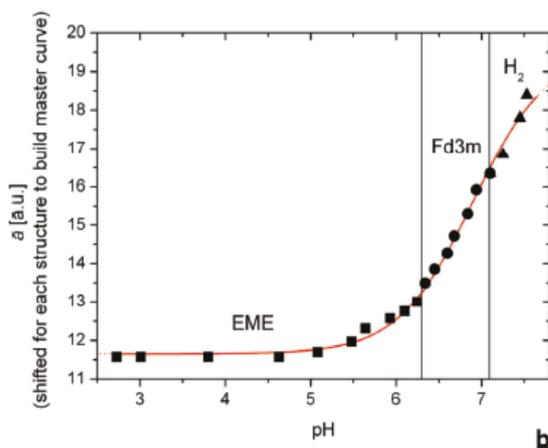
Figure 9: **pH depending lattice parameter** and **structural change** of MO with 80wt% oleic acid. [53]
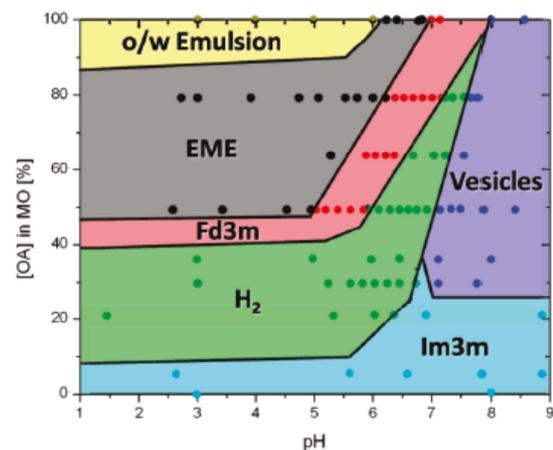
Figure 10: **Phase diagram** of a monoglyceride/ oleic acid system **in dependence of the pH**. [53]

Salentinig expects for systems containing 80wt% oleic acid bicontinuous cubic phases between the inverse hexagonal and the vesicles. As the structure change within this area is extremely sensitive to the pH they were not able to observe this.

Dispersions of monoolein/ oleic acid stabilised by the Pluronic F127 are reported to form the inverse hexagonal phase under acidic conditions and the bicontinuous cubic Pn3m is formed through the pH increase. At neutral pH the cubic Im3m develops. This is explained by the increasing electrostatic repulsion of the deprotonated oleic acid, which leads to an increased effective head group area and therefore favours structures with lower curvatures. Through the addition of salt the Pn3m can be stabilised. [52] [54]

Those dispersions respond on the pH and also different acids can be used. Transition from H_2 to the Im3m was observed by the usage of linoleic acid. Like oleic acid this system is under acidic conditions hexagonal and changes to the cubic phase at pH 7. [55]
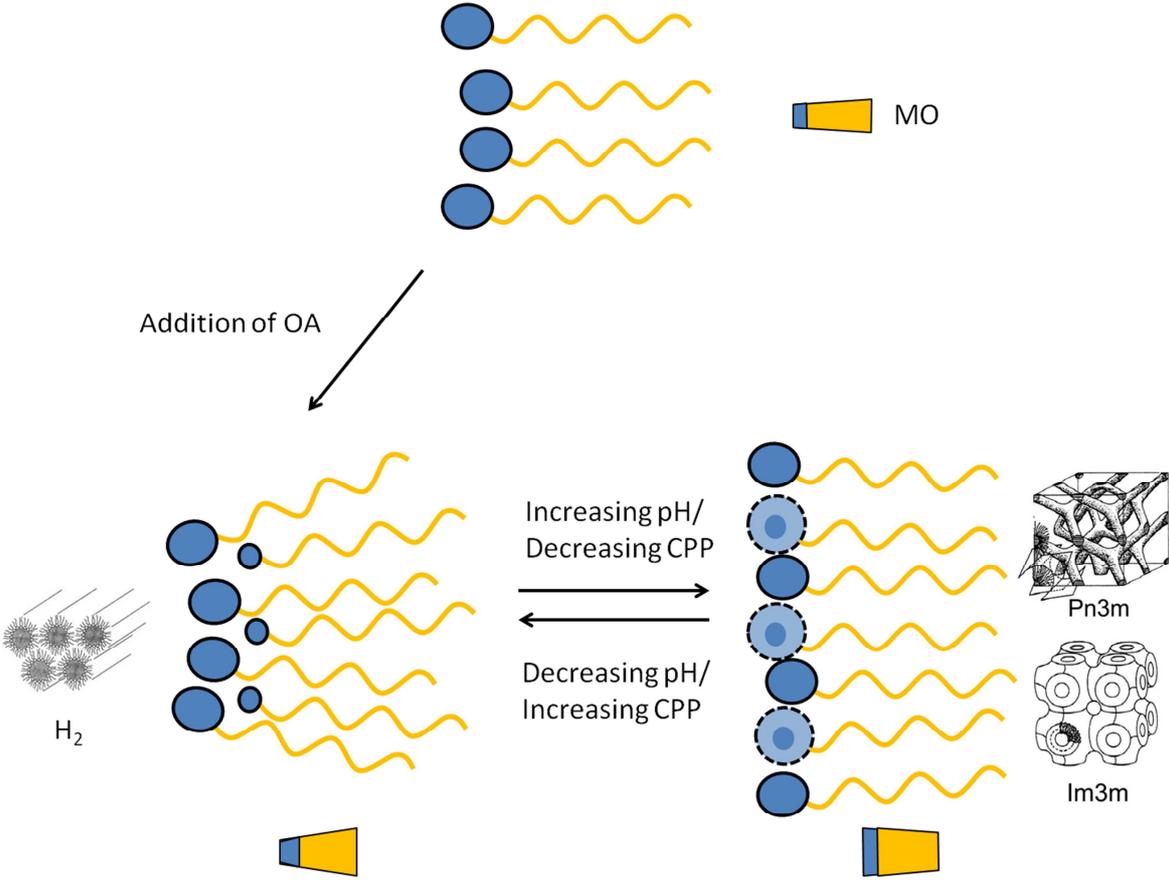
Figure 11: Schematic drawing of the **structure effect of oleic acid** through **pH variation**. After [53] and structure from [64]

Figure 11 gives a schematic overview of the phase behaviour of oleic acid containing systems. Depending on the exact compositions hexagonal phases can be transferred to the cubic Im3m or Pn3m. [21] [55]

A comparative study where ternary systems with monoolein/water and either oleic acid or sodium oleate, have been studied, showed similar phase behaviour. The isothermal phase diagram of monoolein/ water and sodium oleate develops over wide areas lamellar liquid crystalline phases. The lamellar phase was observed even at high water concentrations. Phases containing more than 90wt% water formed stable vesicles. Further inverse hexagonal and bicontinuous cubic Ia3d and discontinuous Fd3m structures were found. The cubic Ia3d destabilized after a few weeks and disappeared. The monoolein/ water/ oleic acid system did not show lamellar phases and was mainly dominated by the inverse hexagonal phase. [31]

Sodium oleate acts as a base so we can expect an increase of the pH. The sodium cations reduce the tension through the high density of negative charges. [54]

This pH behaviour is interesting for our purposes as we can find similar pH conditions within the human digestion system. [56]

2.3.2. Release out of nanostructured materials

The release out of nanostructured materials is mainly depending on the structure, as some arrangements have continuous open water compartments while other structures have enclosed water chambers. [29] [55] [57] Water soluble molecules can be dissolved in the water compartments, while hydrophobic compounds accumulate in the lipophilic area around the surfactants tails and amphiphiles will assemble in the interfacial surface.

Those systems can be loaded with hydrophilic compounds such as proteins [58] and after wards release them. A sustained release is possible if a trigger is built in the nanoparticles like pH depending oleic acid. [55] [59]

3. Methods

3.1. Materials

As a basis for all the experiments Dimodan® U/J from DANISCO Denmark was used. Dimodan® U/J contains 96% of distilled monoglycerides from refined sunflower, raps seed and palm oil. The monoglycerides consist out of 80% oleate, 8% linoleate and 7% saturated fatty acids. Oleic acid from Sigma-Aldrich Germany, with a technical purity of 90%, was another main compound. tetradecane with a purity of 99.0% also from Sigma-Aldrich Germany was used in some experiments either as a substituent for oleic acid, or an additive. Further compounds of the bulk phases or the dispersions were Grindsted® PGE polyglycerol ester O 80/D from DANISCO Denmark (later on mentioned as PGE) and Dimethylsulfoxide (DMSO) 99.0% by Fluka Germany.
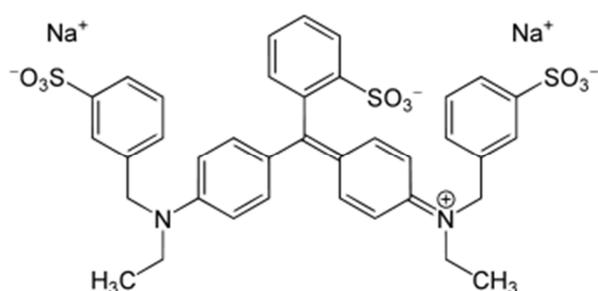
Figure 12: **Anionic Erioglaucine** as dye in the disodium form, for release experiment.

L-Glutamine ReagentPlus® 99.0% (TLC) from Sigma-Aldrich USA, methylene blue hydrate 97.0% from Fluka Germany and Erioglaucine from Sigma-Aldrich Germany were used as additives.
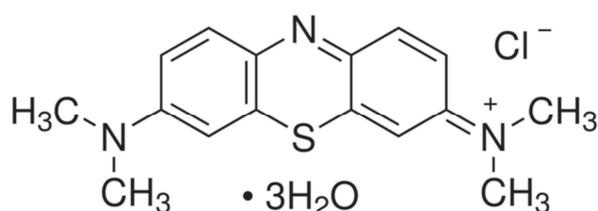
Figure 13: **Cationic methylene blue** in the tri-hydrated form as dye for the release experiments.

To obtain specific pH-values, Sodium Hydroxide 99.0% and sodium dihydrogen monophosphate both from Merck Germany and hydrochloric acid 37% from Sigma-Aldrich Germany were utilized.

The dispersion stabilizer was the triblock copolymer Pluronic® F127 from BASF New Jersey, USA, which we received as a gift. The triblock copolymer consists out of polyethylenoxide and polypropylenoxide and the blocks are ordered as PEO_{99}-PPO_{67}-PEO_{99}. Furthermore distilled water and salt from Saline Austria AG were used. All materials were processed without any further purification.

3.2. Sample preparation

The different properties of the examined samples required diverse preparation methods. The focus of this thesis was on 2 systems, bulk phases and dispersions. The following paragraphs will describe the applied techniques.

3.2.1. Bulk phases

Bulk phases have been obtained via 2 different methods. This was necessary because the simple and fast heating and vortexing method was not suitable for samples containing higher amounts of PGE.

All components for bulk probes have been weighted directly into vials with a Sartorius Analytic A210P-0DI scale. There was no order required for weighting the chemicals in but it turned out to be best starting with Dimodan® U/J followed by the oily phase and finished by water addition. Further additives could either be directly added, if they are liquid, otherwise they have to be dissolved in water first.

To prepare the samples we were referring to the δ-value that is defined as the amount of glyceride over the total amount of glyceride plus oil in percent.

$$\delta = \frac{mass\ of\ glyceride}{mass\ of\ glyceride\ +mass\ of\ oil} 100 \qquad (7)$$

3.2.1.1. Heating and vortexing

The chemicals are mixed in 20mL vials by vortexing (Janke & Kunkel IKA® Labortechnik VF2) and by additional heating, if required. Typically 5 to 10g were prepared. The necessary temperature depends on the δ value of the sample. For best mixing results the temperature in degrees Celsius is the same as the δ value e.g. δ90 demands 90°C. The samples are heated up by a VWR digital heating block and vortexed till they are homogeneous. After those circles of heating and mixing it is best to let the bulk phases equilibrate for at least 1 day at room temperature.

3.2.1.2. Centrifugation

This technique is used for samples containing higher amounts of PGE. Probes with 33wt% of PGE in the Dimodan® U/J basis are heterogeneous if prepared by simple heating and vortexing. The chemicals (2g) are weighted in 4mL vials and then centrifuged with a Heraeus Laborfuge 400R function line for 15 minutes at 25°C and 3000rpm. After this the vials are turned over and centrifuged again. This is repeated till a homogeneous probe is obtained, that is the case after 4-6 cycles.

Centrifugation at higher temperatures (40°C) could be done but for the examined samples no difference could be observed.

3.2.2. Dispersions

Equilibrations of bulk phases are time demanding as the diffusion distance is in the range of mm, therefore dispersions with a few hundred nm diameter were prepared. Compared to bulk phases the diffusion distances are much smaller and therefore the diffusion rate increases. Boyd observed a burst release of loaded nanostructured dispersions. [60] The burst release indicates huge diffusion rates and therefore a faster equilibration could be assumed. Dispersions also have a higher water to particle surface ratio, which accelerates the equilibration.

3.2.2.1. Ultrasonication

Samples with a total amount of 10g were prepared. Therefore 1g of Dimodan® U/J and oil mixtures, according to the δ value were weighted in 20mL vials and 1g of a 7,5wt% F127 solution was added followed by 8g of water. The compounds were roughly vortexed and then ultrasonicated. The ultrasonication was done with a high intensity ultrasonic processor arrangement by Sonics & Materials Inc. Vibra Cell™ VCX 400 and SY-LAB GmbH Pukersdorf Austria. 5 minutes of sonication with 0.5 seconds pulses and 0.5 second breaks at 30% amplitude. Throughout the process the sample temperature increased. Additional heating is possible but was not done.

3.2.2.2. Shearing

Through shearing very homogeneous dispersions with a high oil contend can be prepared. The analysed samples contained 33.3v% oil phase and 66.6v% water. The water solution includes 3.75wt% F127.
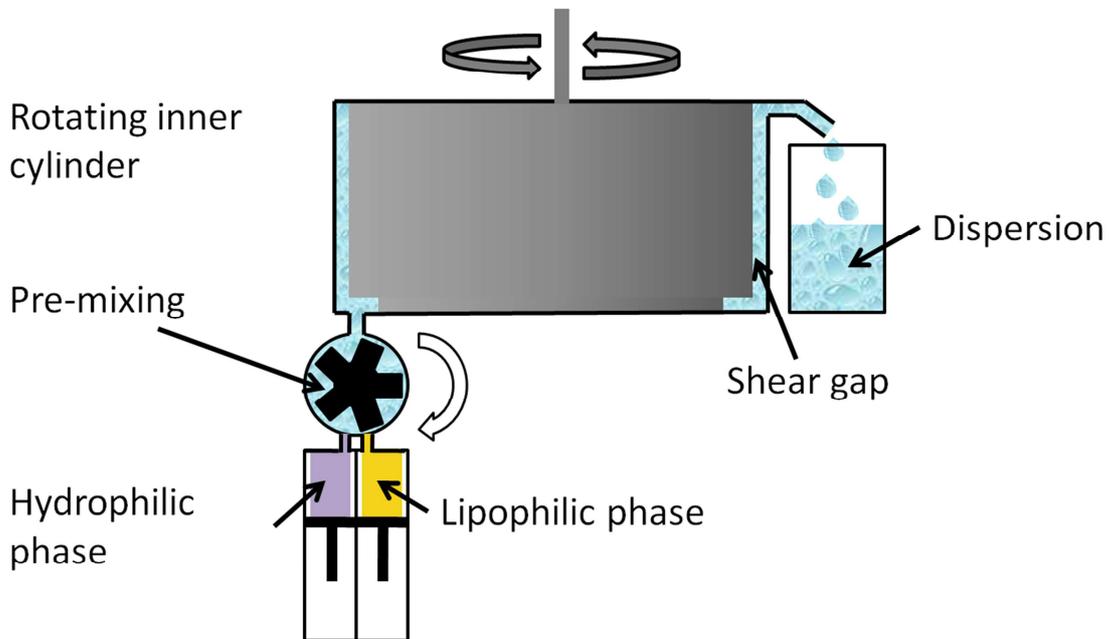
Figure 14: Scheme of the **shearing machine** a with **Couette mixer** [29]

The hydrophilic and the lipophilic phases were filled in 2 storage chambers in volume ratio of 2:1. Via a hand crank both phases were pressed in the premixing chamber, where a crude mixing with a stirrer occurred. The premixer ran at 0.27V and 0.80A, i.e. at relatively low rotation speed. The sample reaches the main shearing chamber above via a small link. The Couette stirrer was set at a speed of 1001rpm. The rotating inner cylinder had a diameter of 60mm and a height of 20mm. Between the inner and the outer cylinder was a 100µm shearing gap. The set parameters led to a shear rate $\dot{\gamma}$ of approximately 31400s^{-1}. To process the requested δ90 samples it was necessary to heat the system up to 90°C.

3.3. Measuring Methods

For the various aspects of the samples, different measuring methods have been applied to analyze them. For the relatively simple release experiments out of bulk phases, UV/VIS spectroscopy was the best choice. To obtain the particle size of the dispersions Dynamic Light Scattering (DLS) was used. The investigation of the internal structure was done by Small Angle X-ray Scattering (SAXS) measurements and additionally by the usage of a polarisation microscope.

3.3.1. UV/VIS spectroscopy

To observe the release of enclosed materials out of bulk phases, dyes were used. The release was analysed with a Hitachi U-3501 UV/VIS double beam spectrophotometer. According to Beer-Lamberts law

$$A = log_{10} \frac{I_0}{I_1} = \varepsilon_\lambda lc \qquad (8)$$

The absorbance A is in a linear correlation with the concentration c. While ε_λ is the molar extinction coefficient and l the length of the cuvette, both are constants. Therefore a calibration line was set up in a series from 0.25 to 10µg/mL for Erioglaucine and for methylene blue from 0.125 to 5µg/mL. The samples have been measured at the absorption maximum of Erioglaucine at 630nm and for methylene blue at 660nm.

3.3.2. Polarisation microscopy
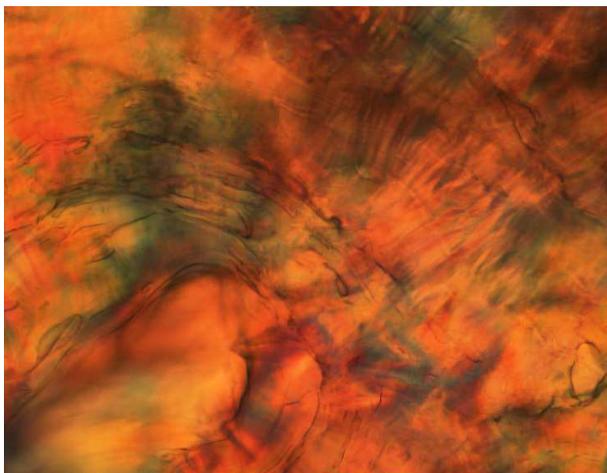
The Leica polarisation microscope DM2500 M was used as an additional method to prove the existence of a hexagonal phase. In transmission mode with crossed polarisers hexagonal phases could be distinguished from cubic phases. While hexagonal phases are changing the polarization, cubic phases do not interfere. This leads to a light transmission.

Figure 15: **Typical microscopy picture** of a **hexagonal water saturated δ90** sample with 6% oleic acid and 4% Tertadecane at pH 4.

The Pictures were taken with a Sony ExwaveHAD 3CCD colour video camera and evaluated with the programme Sarfusoft 2.1 from Nanoline at a magnification of 20:1. The samples have been simply put on standard object slides and were measured at room temperature.

3.3.3. Small Angle X-ray Scattering (SAXS)

To determine the self-assembled nanostructures of the bulk phases as well as the dispersions SAXS was used.

The measurements have been carried out with a SAXSess camera from Anton Paar Austria, which is connected to a Philips PW1730/10 X-ray generator. The generator was operated at 40kV and 50mA with a sealed-tube and a Cu anode. The divergent polychromatic X-ray beam was focused by a Goebel mirror to a line shaped beam of Cu K_α radiation (λ= 0.154nm). To register two-dimensional scattering patterns a PI-SCX fused fibre optic taper CCD camera from Princeton Instruments, a part of Roper Scientific Inc. Trenton NJ USA, was used. The 50mm x 50mm chip has a resolution of 2084 x 2084 via pixel size of 24µm x 24µm at a sample detector distance of 311nm. The working conditions of the CCD detector were at -30°C, which was assisted by a 10°C water cooling. The purpose of the low temperature was to minimize the signal by thermally generated charges. For data
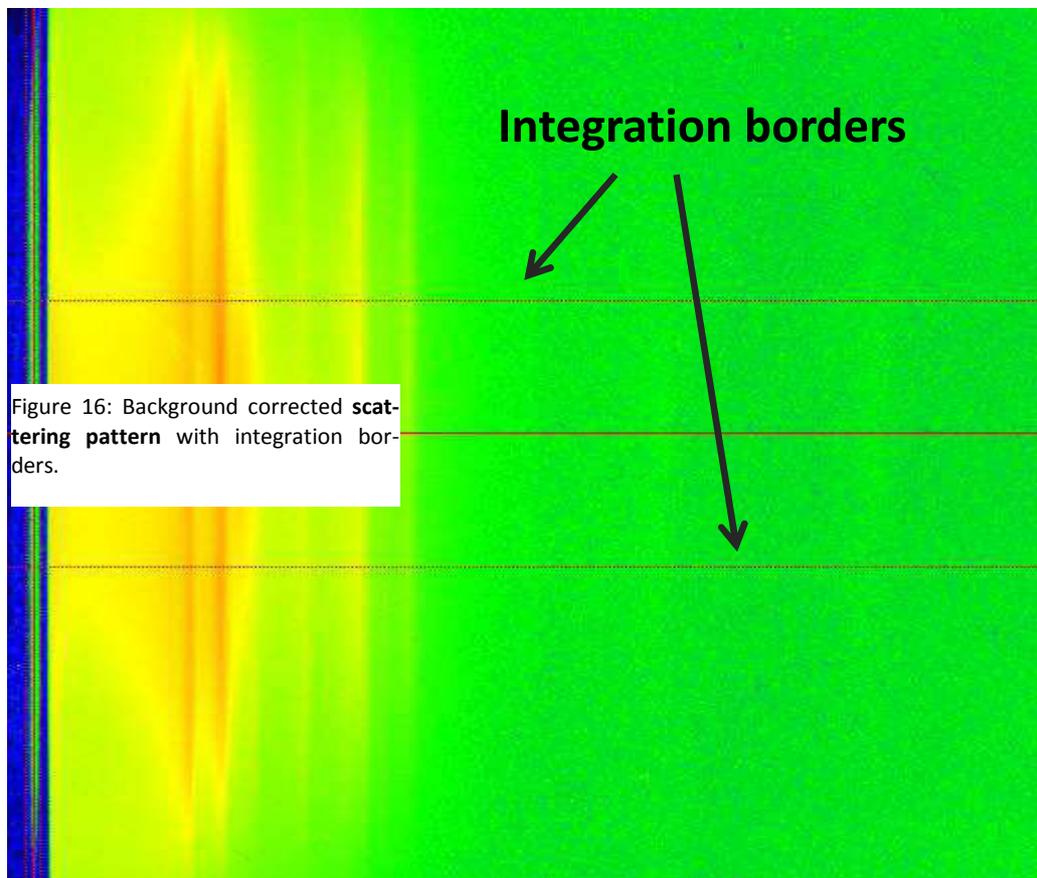
Figure 16: Background corrected **scattering pattern** with integration borders.
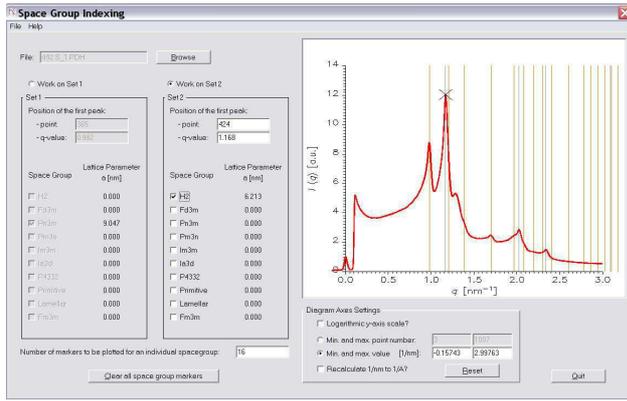
evaluation first the cosmic radiation was subtracted and secondly a background correction was accomplished. A one-dimensional scattering function *I(q)* was obtained through the integration of the two-dimensional scattering patterns. Where q is the scattering vector which is defined as

$$q = \frac{4\pi n}{\lambda}\sin\frac{\theta}{2} \qquad (9)$$

With the wavelength λ, the refractive index *n*, for SAXS *n*=1 and the scattering angle θ.

To define the structures, the peak positions have been determined, because those are corresponding to the reflections of the planes having well-known Miller indices (*hkl*). [23] Each liquid crystalline phase is related to a specific scattering pattern and scattering function *I(q)*.

Figure 17: **One-dimensional scattering function** in the SGI program to obtain the structure.

The Space Group Indexing program SGI (Version 03.2012 by Matija Tomsic) was used for the determination of the structures. The, for this work most important, scattering functions and scattering patterns are plotted on the next page.

Most of the samples were gel like bulk phases, which have been measured in a flat paste cell. Each probe was analysed three times for 2 minutes and averaged. The dispersions on the other hand have been filled in a capillary with a volume of about 100µL. The liquid samples have been measured three times for 10 minutes each. The sample holder included a Peltier element to control the temperature, which was set at 25°C. Temperature scans have been performed for gel like samples with a temperature range from 10-70°C. Each step was recorded three times for 5 minutes with a 10 minutes break to ensure the equilibration.
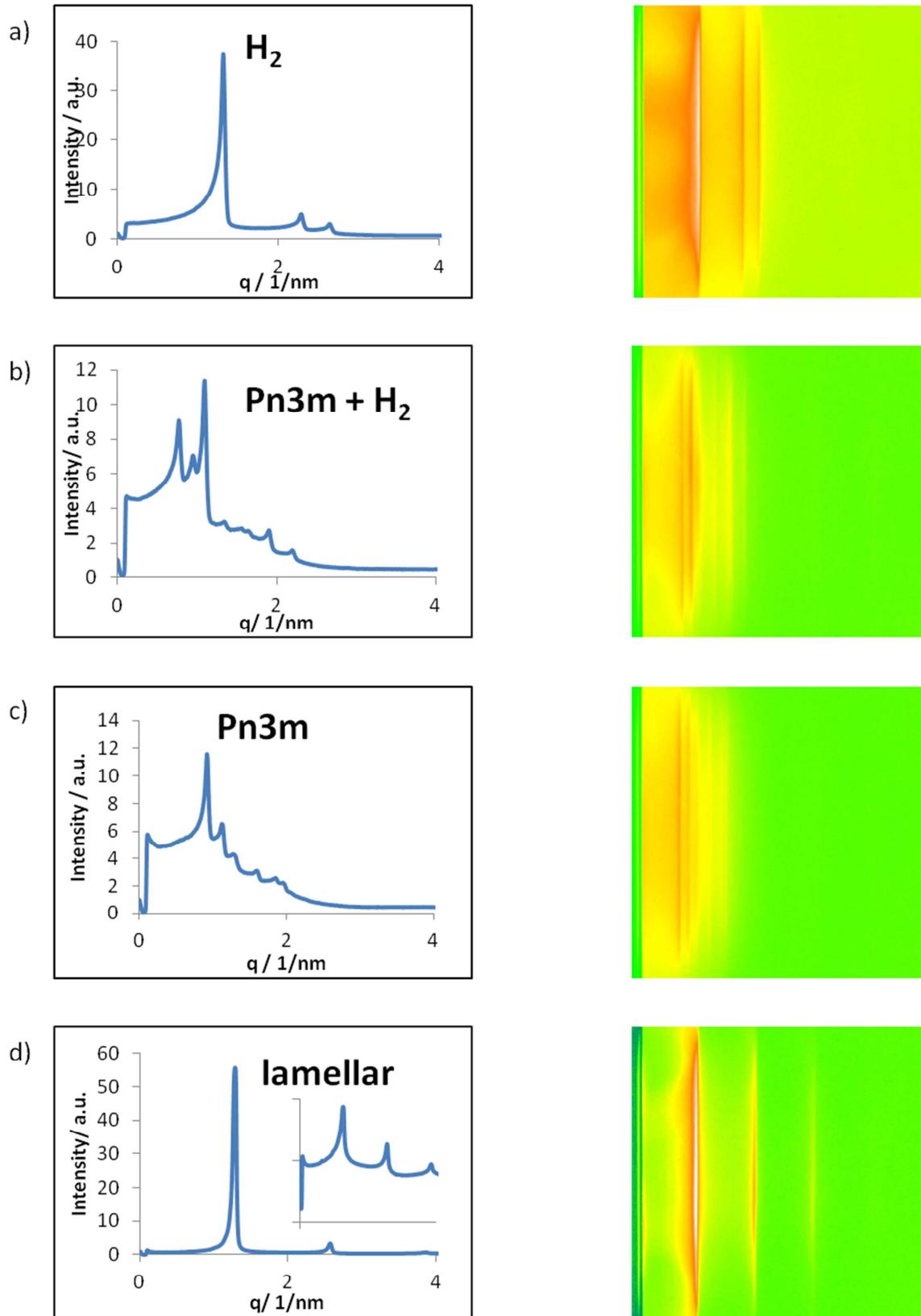
Figure 18: **Scattering functions *I(q)*** and according **scattering patterns**. a) hexagonal **H$_2$**, b) mixture of cubic **Pn3m and hexagonal**, c) cubic **Pn3m** and d) **lamellar** structure the second graph in d) shows the lamellar structure in a logarithmic scale, where the visibility of the peaks is better.

3.3.4. Dynamic Light scattering (DLS)

The particle size of the compounded dispersions, have been measured through DLS

The used DLS instrument consisted out of a laboratory made goniometer and a coherent Verdi V5 diode laser with a wavelength λ=532nm and a maximum power P_{max}=5W. An OZ single mode fibre optics from GMP Zurich Switzerland, was combined with an ALV/SO-SIPD/DUAL photomultiplier with pseudo cross correlation and an ALV 5000/E correlator by ALV Langen Germany.

All measurements where performed at 25°C, an angle θ=90°C and a laser power of 0.15W was adjusted. The temperature was controlled via thermo stated decahydronaphthalene in the index matching bath. To avoid multiple scattering the concentrated turbid dispersions were diluted approximately 1:10000. To dilute the samples, the dispersions have been mixed through handshaking with the corresponding amount of water. Handshaking was sufficient and ultrasonication was not used because particle size changes could have happened.

From the averaged correlation functions of the 10 times 30 seconds measurements the diffusion coefficients D and the hydrodynamic radii R_H have been calculated. The diffusion coefficients and hydrodynamic radii were determined by the cumulant method. [61] Applying the Stokes Einstein relation $R_H = \frac{k_B T}{6\pi\eta D}$ gave the hydrodynamic radii. Where k_b is the Boltzmann constant, T the absolute temperature and η the solvents viscosity.

Preliminary ORT, a software, based on the cumulant method, was used.

4. Experimental and Results

In this section I will describe the experimental details and discuss the results. The phase behaviour of a water/oil mixture is well-known as mentioned in the introduction. First thing done was checking the properties of the nanostructured bulk phases and the structural influence of some additives like salt and dyes were investigated.

We wanted to create systems that change their internal structure through pH variation from hexagonal to cubic. Water soluble compounds should be restrained in the first and rapidly released in the second form.

4.1. Release experiments

The mesophases, L_2 ($\delta 55$), Fd3m ($\delta 70$), H_2 ($\delta 85$) and Pn3m ($\delta 100$) were prepared. The bulk phases were made as describe in the method section. For this samples a basis mixture of 2/3 Dimodan U/J® and 1/3 of PGE was used and tetradecane, as an oil, was added according to
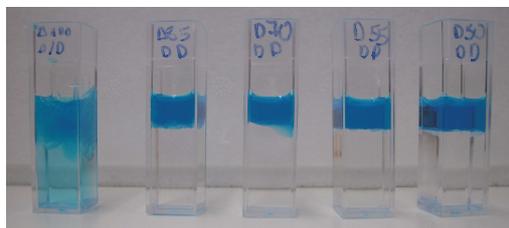
Figure 19: **Tinged bulk phases** with the structures from left to right, **Pn3m**, **H$_2$**, **Fd3m** and **L$_2$**, for photo spectrometer measurements

the δ-value. The release experiments were carried out by the usage of dyes, in our case methylene blue and Erioglaucine. For a time resolved measurement the coloured bulk phases were placed on top of water in the cuvettes, therefore the bulk phases were molten. The used temperature was the same as the δ-value. For example δ70 required about 70°C. δ100 was more challenging, as the bulk phase should have around 100°C and also the water should be as hot as possible. The same technique was used to analyse the release behaviour in the presence of salt or different pH-values. Therefore the water was replaced by corresponding puffer or salt solutions.

4.1.1. Photo spectrometric release experiments

The graphs in Figure 20 show the release of the dye over a period of 25 hours in case of methylene blue and 120 hours in case of Erioglaucine. The dye concentration in water below the bicontinuous cubic Pn3m phase, which we receive with the δ100, increased dramatically after the first few hours. After this fast release the δ100 samples were almost equilibrated and just slight increases occurred.
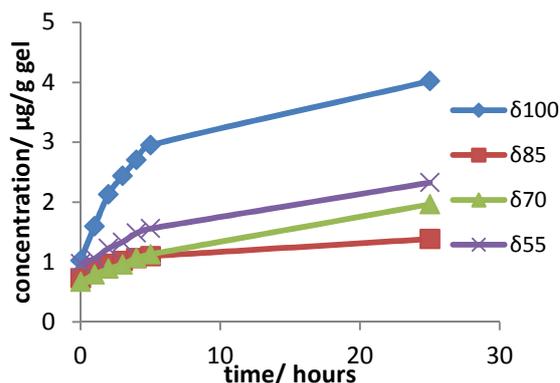
Figure 20: **Time depending dye release** of **methylene blue** out of the different structures
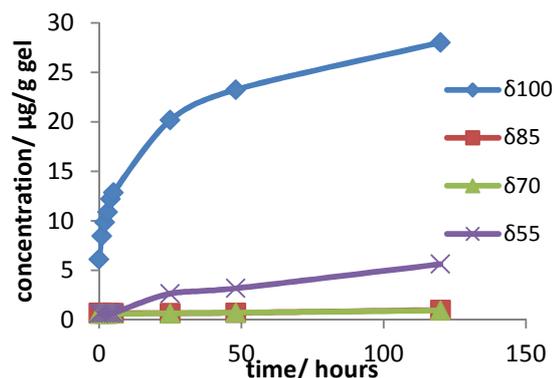
Figure 21: **Time depending dye release** of **Erioglaucine** out of the different structures.

Methylene blue and Erioglaucine behaved similar, in both cases a fast release was observed for the δ100 probes and a significantly slower for the others. Long term measurements over 5 weeks, of especially δ70 with Erioglaucine showed, that almost no dye was released. Compared with the Erioglaucine δ100 the δ70 sample released 280 times less colorant.

The conclusion out of these results is that the water channels of the cubic by continuous Pn3m are connected with the excess water and are therefore leading to a fast equilibration. While the Fd3m, H_2 and L_2 phases restrain the dye, because it is suspected that the water compartments are enclosed within the structure and therefore no direct contact with the excess water is possible. The release also shows that methylene blue is better retained than Erioglaucine. Methylene blue only equilibrates faster, this explains the different time scales, because methylene blue was equilibrated after 25 hours, while Erioglaucine required another 100 hours. After 25 hours for the δ100 samples concentrations of ~2µg/g gel for methylene blue and ~20µg/g gel for Erioglaucine was measured. The dye concentration of 0.1mg/g gel was for both dyes the same.

Furthermore we wanted to know if and how different salt concentrations are influencing the dye release. Loaded δ100 phases in presence of high salt concentrations are releasing the colour much slower than phases without or moderate salt concentrations. The releases of methylene blue and Erioglaucine at 9wt% NaCl are about 3 times reduced compared to the water probes.
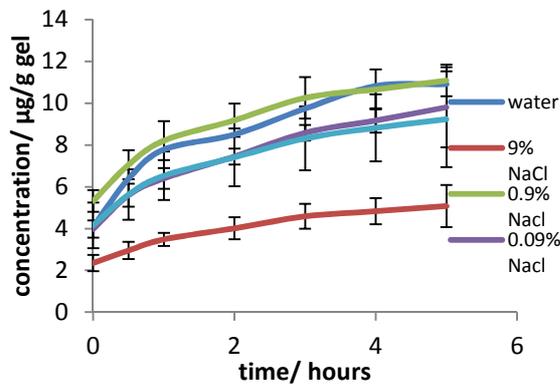
Figure 22: **δ100** with **methylene blue** and various **salt** concentrations
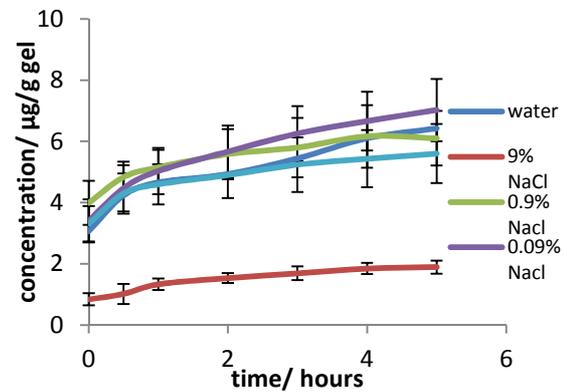
Figure 23: **δ100** with **Erioglaucine** and various **salt** concentrations

Another issue was the pH dependent release. For this question no satisfying answers were found. The bulk phases were exposed to a pH range from pH 3 to pH 11. In case of methylene blue it seems as the release is faster under acidic conditions and is decreasing the more basic the surrounding becomes. The problem was that the noise and therefore the errors were too big to verify this trend. Erioglaucine on the other hand had a quite fast release at pH 3 and pH 11. The pH-values in between showed a slower release.

4.1.2. SAXS experiments
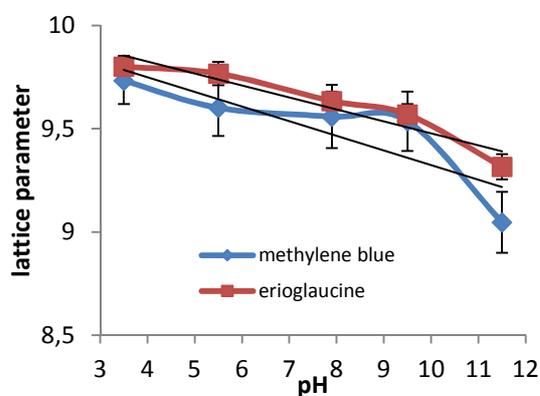
Figure 24: **Decrease of lattice parameters** of **methylene blue** and **Erioglaucine** as a result of the **pH**-value.

Beside the spectrophotmotetric observation of the release, the structural properties of the bulk phases were of great interest. The focus was put on the δ100 bulk phases, which released the dye the best. SAXS measurements determined that the dye loaded δ100 had bicontinuous cubic structures. That was exactly what we expected. The δ100 phases were ana-

lysed with methylene blue, Erioglaucine and without any dye at pH 7.4, the resulting struc-
tures were the same and so were the lattice parameters. Only slight differences in the lattice
parameters of around 9.6nm were observed.

The loaded phases at various pH-values, kept their cubic structure but the peaks were shift-
ing due to a change of the lattice parameters changed. Within the studied pH-range from pH
3 to pH 11 the cubic Pn3m was stable. Methylene blue and Erioglaucine showed pretty much
the same behaviour. The lattice parameters of methylene blue were a bit smaller than those
of Erioglaucine. In both cases we observed a decrease of the lattice parameters when the pH
was increased.
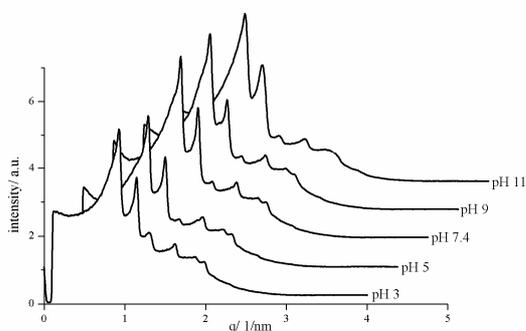
Figure 25: SAXS curves of **methylene blue** at different **pH**-values.
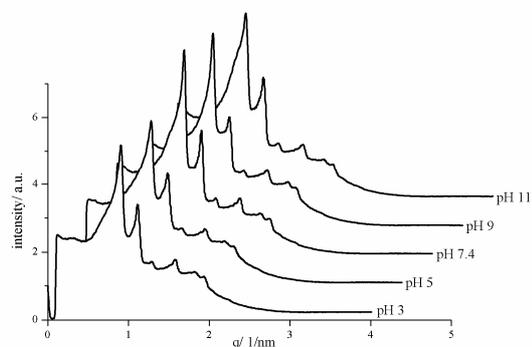
Figure 26: SAXS curves of **Erioglaucine** at different **pH**-values.

With the photometric measurements we realised that bulk phases with a high amount of
sodium chloride had a far less release of the pigments. The examination with SAXS showed
that phases with small amounts of salt have the same structure and even the same lattice
parameters. Methylene blue and Erioglaucine behaved the same way. The lattice parame-
ters of the phases of both colours at 0.09wt% NaCl and 0.9wt% NaCl were close to 9.701
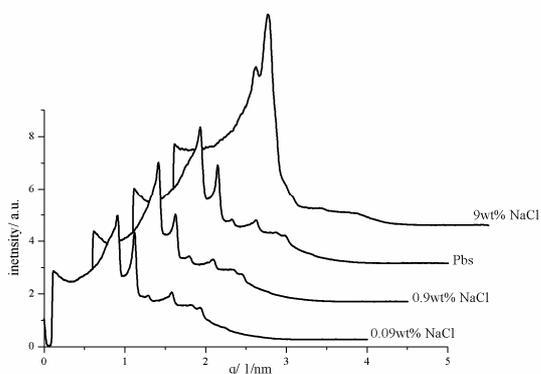
Figure 27: Scattering functions of **δ100** with **methylene blue** with **increasing salt** concentrations.
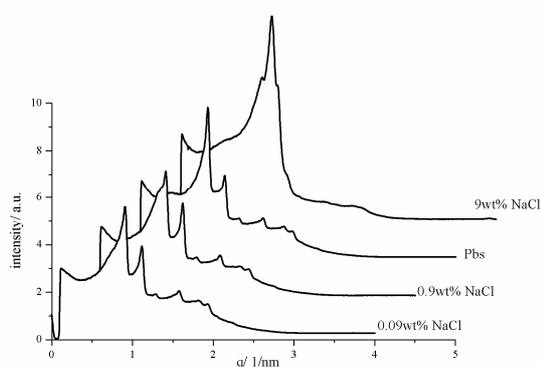
Figure 28: Scattering functions of **δ100** with **Erioglaucine** with **increasing salt** concentrations.

with a standard deviation of 0.075. 0.9wt% NaCl was chosen because it is the physiological salinity. The further increase of the salt concentration led to structural change. A 9wt% salt solution (~1.5M) leads to an increased polarity of the water solution and therefore a reduced solubility of lipophilic compounds. [62] The structure we obtain shows similarities to a cubic Fd3m. This is also fitting to the observation of reduced release out of the bulk phases at high salt concentrations. The release experiments out of different structures clearly reveal that the discharge of enclosed dyes out of the discontinuous cubic Fd3m was significantly inferior, than out of the bicontinuous Pn3m.

4.2. Responsive gels

The intention of the first set of experiments was to get some basic knowledge about the systems behaviour. The influence of salt and pH variation was measured on a model like system. The restrain and release of substances out of bulk phases was observed. The formation of a smart or responsive gel that can transit from a hexagonal phase to bicontinuous cubic phase was the aim.

As described in the introduction, we needed to add a compound to the bulk phases that can respond on an external pH change. All probes of the responsive gel contained therefore oleic acid as oil.

4.2.1. Bulk phases with 1/3 PGE

Based on the phase diagram (Figure 7) and the results of the release experiments, bulk phases were prepared with δ-values from δ85 to δ95 and different water concentrations. The tetradecane that was used in the release experiments to obtain the δ-value was now replaced by oleic acid. The basis mixture consisted out 2/3 Dimodan U/J® and 1/3 PGE.

The preparation of samples with 1/3 of PGE and high δ-values was tricky. Those samples needed to be centrifuged for a long time in to obtain a homogeneous bulk phase.

4.2.1.1. Bulk phases with 1/3 PGE and the influence of water
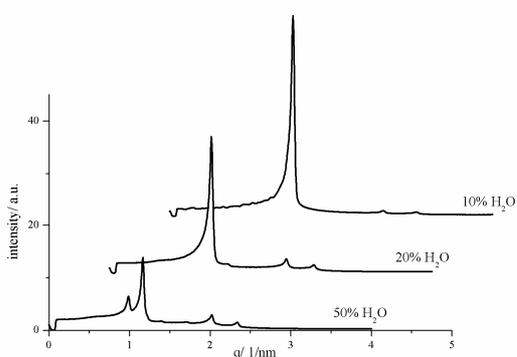
Figure 29: **δ85 bulk phase** with different **water** concentrations. 10% and 20% water are **H$_2$**. 50% water is a mixture of **Pn3m and H$_2$**.

The δ85 bulk phase was hexagonal at low water concentrations but when the water content was increased to 50wt% of the bulk we observed a change towards the hexagonal and the cubic Pn3m phase. This behaviour was not expected, as the tetradecane phase diagram states a pure H$_2$. [41] As we are close to the structural border the different attitude of oleic acid pushes towards the Pn3m.

Parts of the oleic acid are deprotonated and therefore demanding more space compared to tetradecane. Also the protonated oleic acid is acting as an amphiphile through the carbonic acid group and is therefore going closer to the interface. The repulsive forces of the deprotonated oleic acid were changing the curvature, which was indicated by the different structure. We were not able to measure the pH within the bulk phase but derived from the dispersions we can assume a pH between 5 and 6.
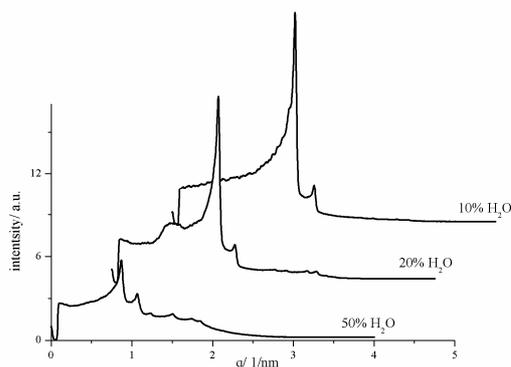
Figure 30: **δ90 bulk phase** with different **water** concentrations. The samples with 10% and 20 % water are cubic **Ia3d** and the 50% is cubic **Pn3m**.

At δ90 the measured structure at low water contents was an Ia3d. When the water amount was increased we observed again a Pn3m. If we compare this with the tetradecane system we would expect a lamellar phase. For all the different δ-values we expect a similar pH range (pH 5-6) if no base is added.

Therefore we can assume that the oleic acid is mainly protonated. The oleic acid is pushing stronger to the cubic phase than tetradecane.

The δ95 bulk phases with 10wt% H_2O formed a lamellar structure, which was recorded through the intense single peak. Increasing the water content to 20wt% led to the cubic Ia3d. Over 50wt% water only the cubic Pn3m was recorded.

Those three δ-values showed that we were close to the well-known phase diagram but through the properties of oleic acid some structural shifts were observed.
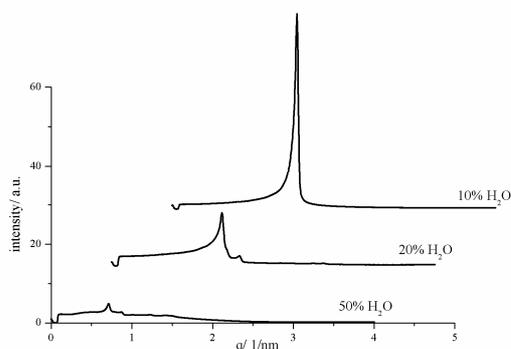
Figure 31: **δ95 bulk phase** with different **water** concentrations. 10% water is lamellar, 20% gives a cubic **Ia3d** and the 50% is cubic **Pn3m**.

If we compare the scattering functions of different δ-values at given water content, we distinguish, that our system with oleic acid is behaving like it has more water compared to the model system with tetradecane.
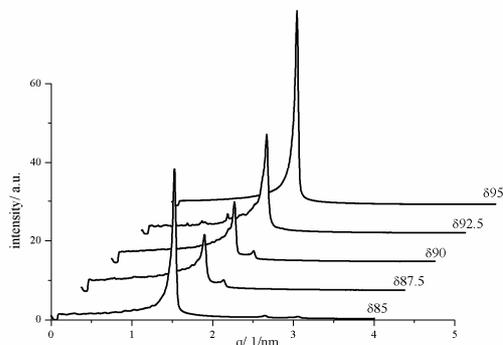
Figure 32: **10wt% water** and different **δ-values. Structural change**s as the result of **oil addition**. δ85 **H$_2$**, δ87.5 and δ90 **Ia3d** and δ92.5 and δ95 **lamellar**.
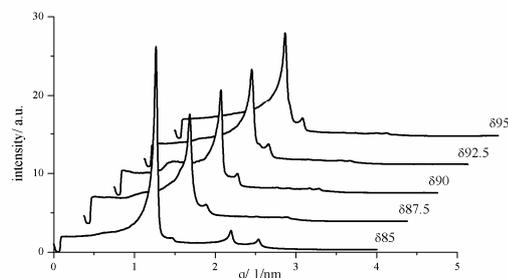
Figure 33: **20wt% water** and different **δ-values. Structural changes** as the result of **oil addition**. δ85 **H$_2$**, δ87.5, δ90, δ92.5 and δ95 are cubic **Ia3d**.

At a 10wt% water amount we got lamellar phases for δ95 and δ92.5, cubic Ia3d for δ90 and δ87.5 and a H$_2$ for δ85. Lamellar would be the corresponding structure of all the bulk phases if tetradecane is used. Our samples with 10%wt water and oleic acid behave more like 15%wt water and tetradecane. With 20%wt water we obtained the cubic Ia3d for δ95 where we still expected a lamellar phase. (Compare Figure 7)
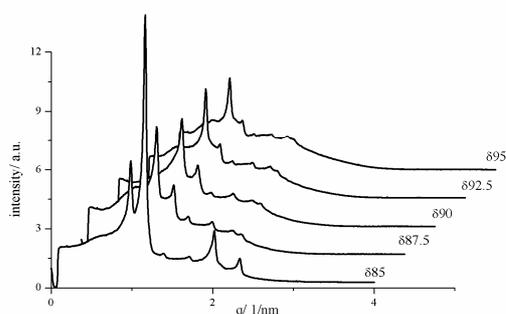
Figure 34: **50wt% water** and different **δ-values. Structural changes** as the result of **oil addition**. δ85 is a mixture of **H$_2$ and Pn3m**. δ87.5, δ90, δ92.5 and δ95 form the cubic **Pn3m**.

The samples with 50wt% water formed just at δ85 a perhaps useful structure. δ85 showed a mixture out of H$_2$ and Pn3m. Under basic conditions this should be a pure hexagonal phase. All other probes were recorded as cubic Pn3m and therefore not suitable for our purpose.

With 1/3 of PGE in the basis mixture only δ85 containing low water amounts was an appropriate candidate for a pH sensitive switchable gel. The δ85 phase was hexagonal with 10wt% and 20wt% water saturation and turned into mixed structures at higher amounts. It seemed to be close enough at the border, to be converted into a cubic bicontinuous phase.

4.2.2. Bulk phases without PGE

As PGE pushes towards cubic phases and the only composition close to the border region with a possible transition from hexagonal to cubic was the δ85 with 1/3 PGE, we decided to process without PGE. The probes consisted therefore only of Dimodan U/J®, oleic acid, water and further additives, if needed. If salt was added, the salinity of the aqueous phase was always 0.9wt% NaCl, the physiological salinity. The preparation of these samples was much easier, because the time demanding centrifugation process was not necessary and the simple heating and vortexing method was applied.

To study the properties of this system we divided the study into two parts. First one was the water unsaturated system and the second one the water saturated. Both series were analysed about their salt dependency and their behaviour through pH changes. The water saturated samples were additionally examined about their temperature dependence.

4.2.2.1. Water unsaturated bulk phases

The following results present the properties of water unsaturated bulk phases in terms of water, salt and base addition.

4.2.2.1.1. Water unsaturated bulk phases and salt dependency

The area around δ90 should be suitable for our purposes. δ90 and δ95 probes were prepared with 10wt% and 20wt% water content, as well as samples with saline water. The salt amount of the water was 0.9%, the physiological salinity.
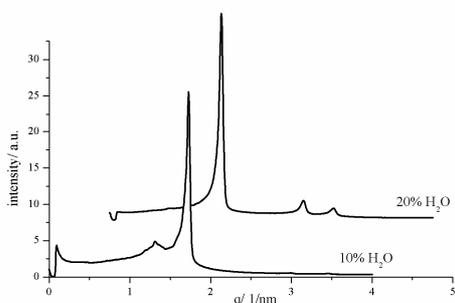
Figure 35: **δ90** with **10wt%** and **20wt% water**. the curve with 10wt% water contains a second structure, which could probably be Ia3d. The **main structure** of both samples is **H₂**.

At δ90 we measured for 10wt% and 20wt% water content a hexagonal phase but the sample with 10wt% water showed an additional signal that probably belonged to the cubic Ia3d. It was not possible to determine to which structure the additional peak in the scattering function belongs. The Ia3d would

be plausible, because the composition this sample is indicating the cubic phase according to the phase diagram. (Figure 5) Also L_2 is likely as it is formed at minor water contents, and the border to the H_2 is close to the 10wt% water amount.

The addition of salt resulted in a shift of the peaks to the left; corresponding to an increase of the lattice parameters from 4.200 to 4.680 for samples with 10wt% water and from 5.251 to 5.349 for 20wt% water. The structure itself was not changed.
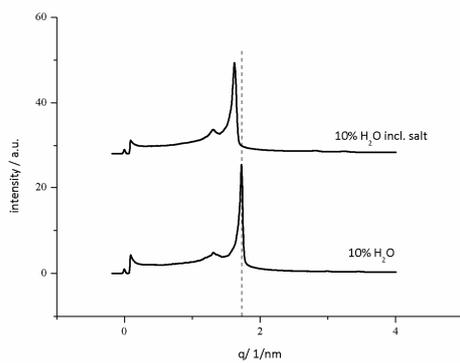
Figure 36: **δ90 observed peak shift** through the addition of **salt** with a **10wt%** aqueous phase.
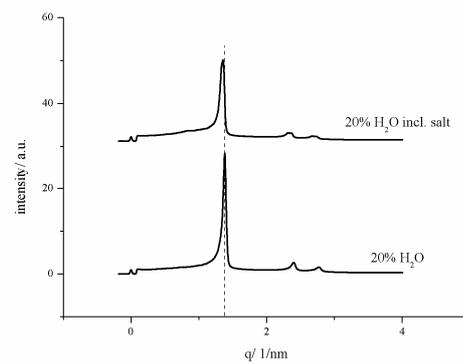
Figure 37: **δ90 observed peak shift** through the addition of **salt** with a **20wt%** aqueous phase.
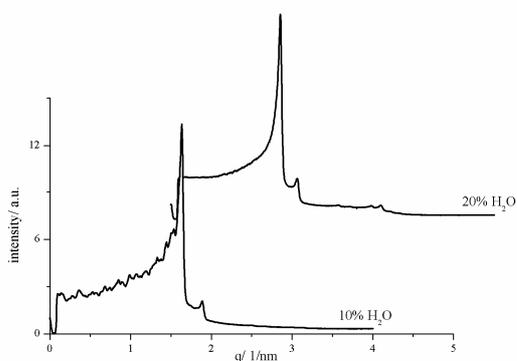
Figure 38: **δ95** with **10wt%** and **20wt% water** amount forming a cubic **Ia3d**.

The δ95 samples resulted in the cubic Ia3d structure for both water contents. The signal quality for the 10wt% water sample and for both salt samples was low. Through the bad quality of the scattering functions no clear shift was observed.

4.2.2.1.2. Water unsaturated bulk phases and pH dependency

To change the pH-value part of the water was substituted by 1M NaOH. Samples with 2.5g each were prepared. 2g consisted of Dimodan U/J® and oleic acid according to the δ- value and the other 0.5g were made up by water, what led to a 20wt% water content. Water was replaced by 1M NaOH in 100μL steps, so we got 6 samples which contained 0-500μL 1M NaOH. These fixed steps were used because we were not able to specify the pH-value within
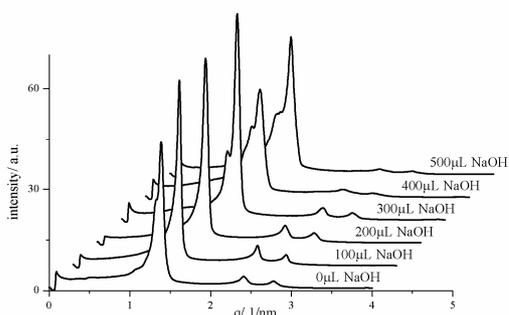
Figure 39: **δ90** with **20wt% water** and increasing **NaOH** amount from the front to the back. **Structural change** from a single hexagonal **to a mixed phase**.

a solid paste. For this set of experiments we chose δ90 as we already observed the hexagonal phase with it. Further samples with the 0.9wt% saline solution instead of water and the physiological phosphate buffer (Pbs) instead of water were prepared.

δ90 without NaOH is hexagonal, when the NaOH content was increased, parts of the hexagonal structure got lost. The sample with 300μL of added NaOH showed already a shoulder on the left side of the H_2 main peak. Further addition of the base led to a broadening of the shoulder. Later experiments affirm that this additional signal belongs to a cubic phase, most likely the Ia3d. A further increase under the given circumstances was not possible as already the whole water content was substituted by NaOH. Increasing the NaOH concentration would also not lead to a satisfying result, because we had approximately the same molar amount of oleic acid and NaOH. So most, if not all, of the oleic acid was already deprotonated.

For these experiments also the salt dependency was examined. The obtained structures were the same as those we got from using plain water. A slight shift of the lattice parameters to higher numbers for salt containing samples was observed but not with a well developed trend.

The water unsaturated bulk phases showed that salt has a minor effect to the structure but there were no structural transitions from H_2 to Pn3m or Ia3d formed as a result of this salt addition. δ90 seemed to be a suitable candidate for the pH sensitive gel. An increase of the NaOH amount led to a structural change, which was observable via the development of a shoulder next to the H_2 peak. As we were not able to receive a cubic phase we decided to have a look on water saturated systems.

4.2.2.2. Water saturated bulk phases.

In view of possible future applications and the dissatisfying results from the unsaturated phases multiple experiments with water saturated bulk phases were performed. Contrary to the unsaturated system we did not find a transition from H_2 to Ia3d but from H_2 to Pn3m. As both, Ia3d and Pn3m, are bicontinuous cubic phases our demands are fulfilled. Also we had already a look on some properties of the Pn3m phase in the release experiments section.

4.2.2.2.1. Water saturated bulk phases and salt dependency

In the same manner, as for the unsaturated phases, we had a look on the influence of a physiological salinity to the structure. Again we used δ90 but in this case with 50wt% and 60wt% water or the corresponding salt solution. In the unsaturated phases we observed a shift of the peak and a therefore resulting increase of the lattice parameter, if salt was added. With the saturated phases no shift was detectable. For the samples with 50wt% aqueous content we obtained exactly the same lattice parameter of 5.987 and also the scattering functions were matching almost perfectly. The same results were received for the 60wt% probes. For those only a slight difference of the lattice parameter was recorded. 5.987 against 6.003 what is within statistical errors.

As a result of no detected differences between samples with and without salt all future samples were prepared without salt.

4.2.2.2.2. Water saturated bulk phases and pH dependency

δ90 samples were prepared by heating and vortexing the ingredients. We used 50wt% water and increased the 1M NaOH content in 10wt% steps in terms of the aqueous phase. After 3 days of equilibration the samples were measured with SAXS.

Without added NaOH we recorded the H_2. When the amount of the base was increased also
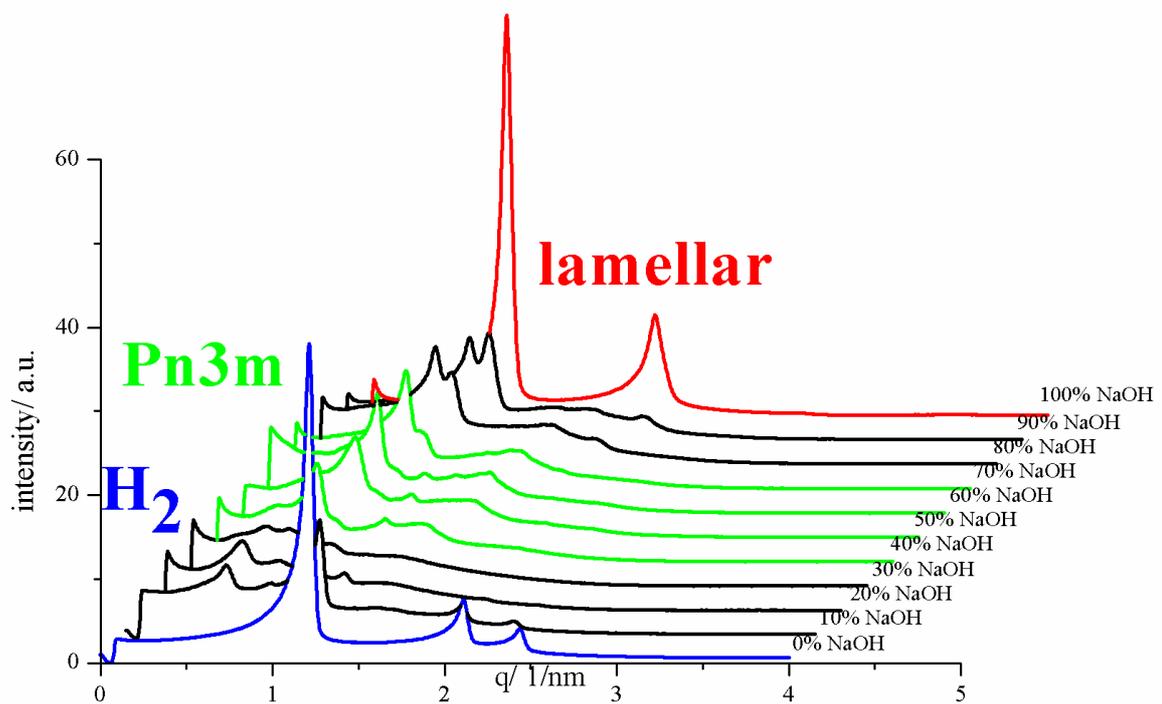
Figure 40: **δ90** with increasing amounts of **NaOH**. **Structural changes** are observed **from H_2 via Pn3m to lamellar**. The **green** scattering functions plot the area were the **desired Pn3m** is found.

the structure changed. Through the first steps the signal of the hexagonal phase decreased rapidly but was still observable. Between 40% and 70% of added NaOH the obtained structure had similarities to the Pn3m and no hexagonal structure was detected anymore. This Pn3m like structure was not as well developed as we hoped. A further increase of the NaOH content led to an additional structural change. First another peak appeared next to the Pn3m main peak that belonged to the lamellar phase. Finally just the lamellar phase was left. Figure 40 plots the desired structures in green. As we are not satisfied with this not pure Pn3m we decided to have closer looks on two additional parameters, temperature and oil content.

To start with a distribution of the oil content we analysed samples with δ-values from δ88 to δ92 in 1% steps. The addition of NaOH was the same as for the already characterised δ90 sample. Through the addition of NaOH a structural change of all probes was recorded. A problem was the preparation of homogeneous samples. All in all 3 sets of samples were made via different preparation methods. We used the heating and vortexing method as well as centrifugation at 40°C and 20°C.

The results of the measurements were fluctuating. If we take for example δ89 with no NaOH added it was always hexagonal, when the NaOH content was increased to 10% it showed a dominating Pn3m and less H_2 but a further increase to 20% resulted in a dominating H_2 and a minor signal of the Pn3m. Fluctuations like this were observable over the different preparation methods as well as for different δ-values.
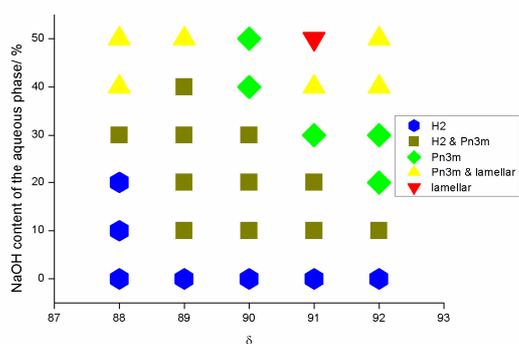
Figure 41: **Phase diagram** of **water saturated** bulk phases. **δ against NaOH** content. The colours indicate the different structures and the **desired structures** are marked **green**. The starting structure H_2 is blue and the unwanted lamellar red.

Figure 41 shows therefore a condensed semi-qualitative phase diagram of δ-values against NaOH content. We can observe a trend, that more NaOH is needed to change from the H_2 to the Pn3m, if the δ-value decreases. The explanation is the increasing amount of oleic acid that is added to the bulk phase. More oleic acid need more NaOH to compensate its acidity. We can also see that all analysed samples are suitable for a structural transition. In the case of δ90 we were lucky and obtained a quite pure Pn3m. Also we observed that a too high increase of NaOH was leading to lamellar structures. Experiments for δ90 with smaller NaOH steps led to the same result as above. Also those finer increments did not lead to better resolution of the structural transition.

4.2.2.2.3. Water saturated bulk phases with tetradecane

Tetradecane was used in earlier experiments as a model like oil. Also literature is referring to it often. [20] [32] [37] As tetradecane has no head group that is sensitive against a pH change it is not suitable to substitute the whole oleic acid against it. But as we experienced already nice results with tetradecane
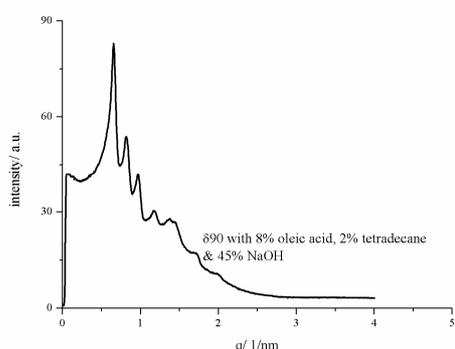
Figure 42: Scattering function **of δ90 with 8wt% oleic acid, 2wt% Tetradecane** and **45% of NaOH** in the aqueous phase. **Pn3m** as the structure was determined.

we took our quite well working δ90 and replaced 20wt% of oleic acid by tetradecane. The composition of the new sample in the lipid phase therefore was 90wt% Dimodan U/J®, 8wt% oleic acid and 2wt% tetradecane. As we worked in the saturated area we had a water content of 50wt%. To this sample NaOH was added in 5% steps and at a NaOH content of 45% we obtained a pure Pn3m.

4.2.2.2.4. Water saturated bulk phases and temperature behaviour

The samples from the pH-dependency experiments were also analysed about their temperature behaviour. These samples consisted of Dimodan U/J®, oleic acid, water and NaOH. Therefore we measured temperature scans from 5°C to 60°C in 5° steps and an additional point at 37°C.
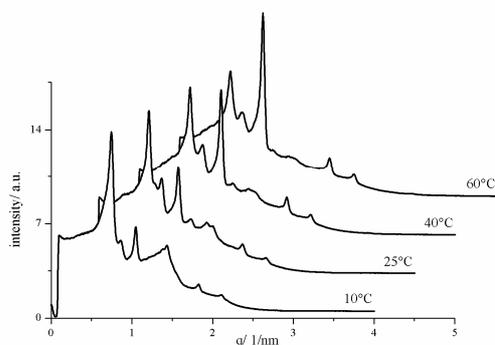
Figure 43: **Temperature scan** of **δ90** and **40% NaOH**. Through the increased temperature the cubic phase is forced back and the hexagonal is emerging.

Samples with low NaOH amounts showed at low temperatures a signature of a cubic structure depending on the composition. An increase of the temperature result in a decrease of the Pn3m signal and an increase of the H_2 signal. This is according with the results of temperature depending phase diagrams of similar systems. [2]

In case when a higher amount of NaOH was used, the Pn3m structure did not disappear completely but its formation was weaker. At temperatures around 60°C H_2 is the dominating phase. Another aspect we gained was the temperature stability. It turned out that the samples were keeping the same structure at low temperatures as they had at room temperature, a fact that might be important for long term storage. Further the structure change through temperature variation is reversible.

4.2.2.2.5. pH dependency with salt

The results from the pH variation experiments showed that we were able to get Pn3m like structures but it was hard to get a pure Pn3m. We observed at the water unsaturated samples just a minor influence of the appearance of salt and water saturated probes showed exactly the same behaviour when we did not change the pH-value. Samples with salt and different NaOH contents were prepared to prove a salt dependency, as salt might help to form clearer structures. The samples contained Dimodan U/J®, oleic acid, water, salt and base.

δ90 was used to analyse the influence of salt. For this kind of sample we hardly could see a different behaviour. At low amounts of added NaOH we had the hexagonal phase and when the base content was increased we observed again mixtures of Pn3m and H_2. With salt we were also not able to obtain pure cubic structures.
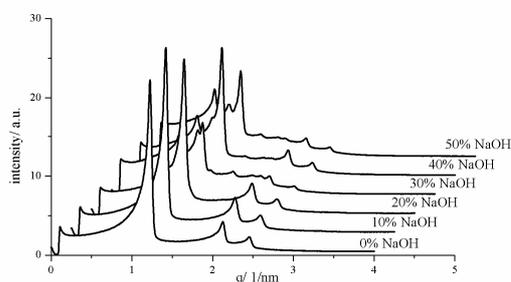
Figure 44: Behaviour of a **salt containing δ90 against a pH** variation.

The hexagonal phase was more stable in the presence of salt, because up to 20% of NaOH content it was the only appearing structure. Also when the base amount was further increased the H_2 peaks did not disappear completely. It seems as salt is stabilising the hexagonal structure. The increased polarity of the aqueous phase is reducing the solubility of the oleic acid and pushes it more into the lipid

phase were it is shielded from the base and the therefore resulting deprotonation. Deproto-nated oleic acid is shielded by the sodium ions, therefore the repulsive forces are weaker and the effective head group area is smaller compared to salt free systems.

The samples from δ88 to δ92 were all suitable for an applied structural change through a pH variation. The desired cubic structures were repeatedly found but the quality was not satis-fying enough. We also figured out that salt has a no detectable influence if no pH change is performed but when we vary the pH we can see differences. Salt within a pH variation stabi-lises the hexagonal phase.

The phase diagram with various δ-values against NaOH amounts shows that we can find 3 structures, hexagonal, cubic and lamellar. Also we can see that there is a quite large area where the cubic structure is stable.

As an additional tuneable parameter we introduced tetradecane, which substituted small amounts of the oleic acid. We found a perfect Pn3m with a δ90 8wt% oleic acid, 2wt% of tetradecane and a NaOH content in the water phase of 45%.

At low temperatures (5-10°C) the structures, which also occur at room temperature, were found, while heating the samples up led to an increase of the hexagonal phase.

4.2.3. Floating bulk phases

As we were able to produce samples which change their internal structure through a pH variation, we focused on a fine tuning. Through the direct addition of NaOH to the bulk phase we observed the desired change to the cubic phase but in hardly any sample it was of a satisfying quality. As the fine pH variation with the bulk phases is hard to manage, a new kind of experimental set up was created.
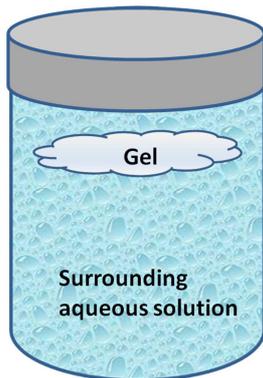
Figure 45: Schematic sample preparation of **floating bulk phases**.

In a first step the lipid phase was prepared with all its additives, except those dissolved in water like NaCl, NaOH and the glutamine. The lipid phase was mixed by heating and vortexing and afterwards 1mL (~0.75g) were pipetted to a 20mL glass vial with 20mL of water or a corresponding saline solution. The lipid phase form there a cloud or sponge like bulk phase. The vials were closed and the samples equilibrated for a minimum of 3 days at 25°C. Through the equilibration in the aqueous solution the bulk phase is water saturated.

This method had the advantage, that several sensitive tuning parameters could be screened. We changed for example the salinity by dropping the lipid phase to a saline solution. pH variations were utilised by adding NaOH to the water and shaking it. Another advantage was that the pH- value could be measured with a glass electrode. When the pH was adjusted further time for equilibration was necessary, for each adjustment 1 day minimum.

Through the before obtained results bulk phases with various compositions were studied. Additives such as PGE, DMSO as well as glutamine were used for sample preparation.

4.2.3.1. Floating bulk phases with various compositions in water

Samples with delta values from δ85 to δ95 were prepared with various additives and equilibrated in water. We had several sets of samples. One contained only Dimodan U/J®, oleic acid according to the δ-value and water. Others contained 10wt% of DMSO or PGE in the Dimodan U/J® basis and another series replaced up to 1/3 of the oleic acid by tetradecane. To all these samples NaOH 1M was added in 20µL steps.

After the equilibration the samples were analysed and should show a structural change. The outcome was that no desired structural change was observed. Only δ90 with 90 wt% Dimodan U/J®, 8wt% oleic acid and 2wt% tetradecane developed a cubic structure with a bad signal at pH ~7. It was checked if the different preparation method had an influence but by comparing the results out of the saturated bulk phases without NaOH and NaOH free floating samples no difference was observed. Both were water saturated and showed at a given composition the same structure.

When NaOH was added the saturated phases changed their structure and the floating phase did not. Per gram we added to both series the same amount of NaOH. In case of the saturated bulk phases each 20µL of substituted base was dissolved in 1g water, while in the floating gels 20µL of NaOH were diluted in 20g water. This made a dilution factor of 20. In the saturated bulk phases the concentration of dissolved base and therefore the concentration of ions was higher compared to the floating phases. The higher concentration within the water phase could affect the structural transition process.

To increase the ion concentration in the floating phases, salt was added. The new samples were floating in a solution with a salinity of 0.9wt%.

4.2.3.2. Floating bulk phases in saline solution

As described above it was necessary to produce salt containing samples. The new measurements recorded huge differences. All samples described in the following subsections were floating in a 0.9wt% NaCl solution.

4.2.3.2.1. Floating bulk phases with diverse δ-values

Bulk phases from δ85 to δ95 were used. Through the equilibration in the saline solution structure changes were observed. All samples were, before NaOH was added, hexagonal except for δ95 which was already cubic. The starting pH-value was between pH 5.5 and 6.2 depending on the amount of oleic acid. The general trend was observed that the pH was increasing when the δ-value increases, which automatically meant a decrease of the oleic acid content.
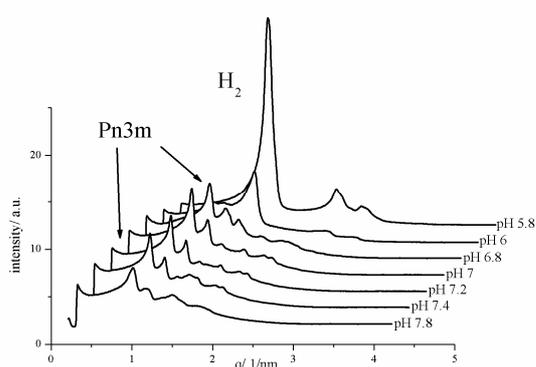
Figure 46: **δ90** with increasing pH from the back to the front. **Structural change** from hexagonal **to cubic** around **pH 7**.
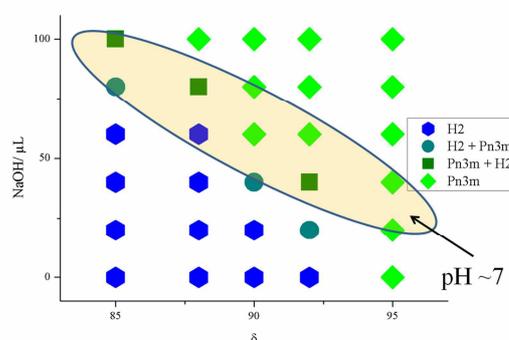
Figure 47: **Phase diagram** of **floating gels**. Different **δ**-value against **NaOH** content. Samples with low δ-value need more base to convert to the Pn3m.

δ90 for example showed a smooth transition from H_2 to Pn3m. At the starting point at pH 5.8 H_2 is the only visible structure and the scattering function had a huge intensity. When base was added the intensity of the H_2 signal was reduced and from pH 6.8 on the cubic Pn3m was observable. Between pH 7 and pH 7.4 Pn3m was the only recorded signal. Increasing the pH further led to increasingly smeared scattering function. The pH was not incremented over pH 8 as we expected there the lamellar phase, which we have observed at the saturated bulk phases.

Similar to the saturated bulk phases we can plot a phase diagram for the floating gels. The needed amount of NaOH to convert the H_2 into a Pn3m was increasing with the decrease

of the δ-value, because more oleic acid must be compensated.

Between the pH-value from pH7 to pH 7.4 the structure transition took place. This was valid for all samples and is connected with the behaviour of oleic acid. [53]

As δ95 was at the starting point already cubic, it was not a suitable sample for the structure transition.

A look at the lattice parameter showed that in increase of the NaOH content led to an increase of the lattice parameter. The extended amount of deprotonated oleic acid required more space and therefore enlarges the unit cell which is represented by the lattice parameter. The same thing was observed when the parameters of the different δ-values were compared. As Dimodan U/J® occupies more room and has a different curvature from oleic acid the lattice parameters were increasing with the δ-value.

H_2/ Pn3m lattice constants						
δ/NaOH	0	20	40	60	80	100
δ85	5.583	5.650	5.678	5.851	6.298/ 10.264	6.470/ 11.201
δ88	5.671	5.836	5.777	6.147	6.066/ 10.454	10.629
δ90	5.732	5.895	6.147/ 9.569	10.081	10.858	10.956
δ92	5.911	6.163/ 9.106	6.213/ 9.106	9.135	9.075	10.692
δ95	8.659	8.659	8.877	9.106	9.601	10.100

Table 2: **Lattice parameters**. **δ**-value against **NaOH** addition. The colour indicates the structure. **Blue H_2, greenish H_2 and Pn3m** mixtures and **green Pn3m**. For mixed structures both parameters are printed, where the value after the / belongs to the Pn3m.

4.2.3.2.2. Floating bulk phases with PGE and different δ-values

As we already know PGE is forcing the gels towards the cubic phase. Therefore we studied this behaviour under the influence of pH variation. As too high amounts of PGE were not satisfying in previous experiments the PGE content was fixed at 10wt% of the monoglyceride phase.
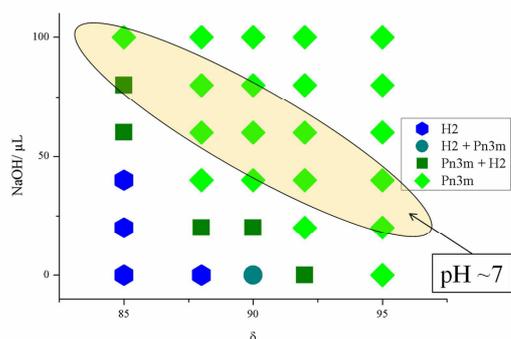
Figure 48: **Phase diagram** of **floating bulk phases** with **10wt% PGE**. the **transition** from H_2 **to Pn3m** is **shifted** to **lower NaOH** amounts compared to the phases without PGE.

These samples were prepared and treated the same way as the floating bulk phases without PGE.

The resulting phase diagram shows a structural transition at lower NaOH addition. The area around pH 7 is indicating the conditions were the change occurred for the samples without PGE. We observed through the addition of 10wt% PGE that the structural changes took place at lower pH-values. The lower pH is explained by the lesser amount of needed NaOH. The oleic acid content was the same as in the previous samples.

As we already observed PGE is more space demanding and reacts therefore more sensitive to the deprotonation process of the oleic acid. PGE itself is turning towards the Pn3m, therefore small changes in the protonation of state of oleic acid are leading to the cubic structure.

The higher δ-values δ90 and δ92 were already mixed phases at the starting point. An increase of the pH led again to pure cubic structures. Also for δ90 we were able to obtain the hexagonal phase when the pH was decreased by the addition of HCl.

At this composition δ85 and δ88 are the most promising samples. The pH at which the structure changed was around pH 6.8. The addition of PGE gave us the possibility to vary the pH-area in which the phase transition takes place. The possibility of lowering the pH-value is increasing the range of future applications.

Comparing the lattice parameters led to similar observations as before. An increase of the pH is enlarging the lattice parameter as well as the increase of the δ-value. Only the lattice parameters of the Pn3m are fluctuating a bit but also these samples showed the same trend.

4.2.3.2.3. Floating bulk phases with different PGE contents

As PGE containing samples led at lower pH-values to cubic phases, we wanted to investigate this behaviour in more detail. Therefore δ90 samples with a PGE content of 0wt%, 10wt%, 20wt% and 33wt% were produced.
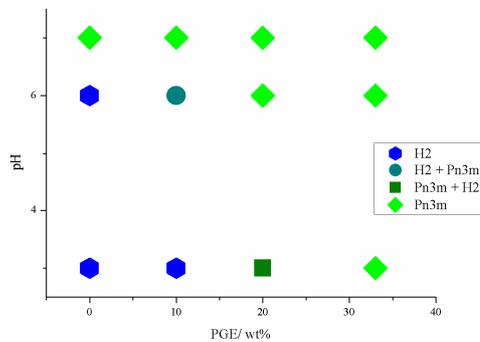
Figure 49: **Phase diagram** of **d90** samples with **increasing PGE** content against the pH-value. Higher PGE amounts require more acidic conditions.

As the δ-value for all samples is the same, also the content of oleic acid is the same. Therefore we can directly compare the behaviour at specific pH-values. The amount of NaOH needed to obtain a specific pH was the same for all samples.

Increasing the PGE content led to the Pn3m already under the starting conditions of pH 6. When NaOH was added to receive pH 7 all samples transferred to the cubic phase. As the samples containing 20wt% and 33wt% were cubic at the starting pH of 6, HCl was added. At pH 3 the sample without PGE was hexagonal as well as the sample containing 10wt% PGE. The 10wt% probe showed at pH 6 already partly cubic patterns but through the increase of the $[H_3O]^+$ concentration it was converted to H_2.

The 20wt% sample developed partly the hexagonal structure but the cubic was dominating. The further increase of PGE to 33wt% just led to the Pn3m. H_2 was not observed for this sample at any pH.

Increasing the PGE content also led to a rise of the lattice constants. Like the other samples, this series showed increased lattice parameters through the addition of NaOH.

H$_2$/ Pn3m lattice constants			
PGE / pH	3	6	7
0wt%	5.732	5.895	10.081
10wt%	5.889	6.147/ 8.659	10.629
20wt%	6114/ 8.606	9.047	11.615
33wt%	10.190	10.856	14.933

Table 3: **Lattice parameters**. **δ90**-with different amounts of **PGE** against the **pH**-value. The colour indicates the structure. **Blue H$_2$, greenish H$_2$ and Pn3m** mixtures and **green Pn3m**. For mixed structures both parameters are printed, where the value after the / belongs to the Pn3m. An **increase of the lattice constants** is observed through the addition of **PGE and/ or** the rise of the **pH**-value.

The addition of PGE led to a structural conversion at lower pH-values. When the PGE content was increased to 33wt% no transformation was recorded. δ90 with 20wt% PGE partly developed the hexagonal phase. Comparing these results with the phase diagram of different δ-values and 10wt% PGE, we can assume that samples with δ85 and 20wt% PGE could form the H$_2$ at lower pH-values

On the other hand samples with a higher δ-value will not be suitable for a responsive gel, as they will be cubic also under acidic conditions. The maximum amount of PGE where the gels show a responsive behaviour is between 10wt% and 20wt% PGE depending on the δ-value. We can assume that δ85 with 20wt% PGE is a suitable responsive gel, because this phase requires an increased deprotonation of the oleic acid for the structural transformation and PGE is pushing towards the cubic phase. 10wt% PGE was the observed maximum for δ90 as already more acidic conditions were necessary to form the hexagonal phase. The maximum PGE content could be increased close to 20wt%. This requires on the other hand lower pH-values around pH 3.

4.2.3.2.4. Floating bulk phases with DMSO and different δ-values

Through the polar aprotic and kosmotropic behaviour of DMSO and its miscibility in organic solvents as well as water and the observed reversed manner of DMSO compared to glycerol in mono olein (42), we were expecting the opposite behaviour to that of PGE. The samples were prepared in the same way as the PGE probes this means a basis mixture of 90wt% Dimodan U/J® and 10wt% DMSO was prepared. The basis was mixed with oleic acid according to the δ-value and was then dropped in the 0.9wt% NaCl solution.

The phase diagram reflects the expected behaviour. Increasing the DMSO content to 10wt% requires higher amounts of NaOH to perform the structural transformation. With 10wt% DMSO 100µL NaOH were needed compared to 60µL NaOH in the DMSO free phase.
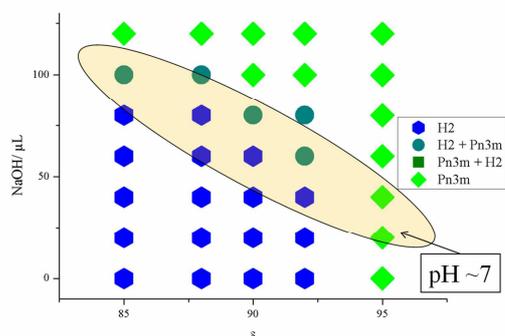
Figure 50: **Phase diagram** of **floating bulk phases**. Different **δ**-values against the **NaOH** content. With **10wt% DMSO**. **Opposite to the PGE samples** the required pH to receive the Pn3m is shifted to higher values.

From the beginning on the δ95 was again cubic. All so far analysed δ95 water saturated and floating samples were cubic, no matter which additives they contained or what pH was selected. We therefore can conclude that δ95 is not a practicable composition for the responsive gel.

We were able to convert all samples to the Pn3m but more NaOH was required compared to the samples described before. In total 120µL of 1M NaOH was added to obtain the cubic structure. To the samples with PGE and without any additive only 100µL 1M NaOH were pipetted. The transition from hexagonal to cubic occurred for the δ90 at pH7.5 and therefore about 0.5 pH-units higher than the sample without DMSO.

4.2.3.2.5. Floating bulk phases with different DMSO contents

As 10wt% of DMSO in the lipid phase of our samples increased the amount of NaOH needed for the structure transition, a further increment of the DSMO should lead to the cubic phase at even higher pH-values. δ90 samples with 0wt%, 10wt%, 20wt% and 33wt% DMSO were prepared.
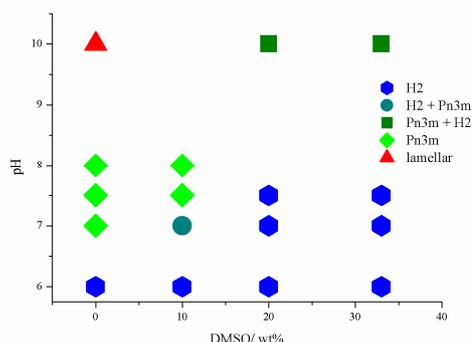
Figure 51: **Phase diagram** of **δ90** with different amounts of **DMSO** against the **pH**. **Structural changes** were observed at **higher pH**-values compared to the DMSO free δ90.

We recorded, as expected a shift to higher pH-values for the structural conversion. The diagram displays the found structures at a given pH. The δ90 samples with 0wt% and 10wt% DMSO responded between pH 7 and pH 7.5. When the DMSO content was enhanced to 20wt% only the hexagonal phase was observed under physiological conditions. It was necessary to adjust the sample at pH 10. There the Pn3m was present but also the H_2 still was visible. The same thing happened with the sample containing 33wt% DMSO. At pH were we got the Pn3m with higher amounts of DMSO, the sample without the additive was already lamellar.

Comparing the lattice constants did not give such a clear trend as for the samples with PGE.

H_2/ Pn3m/ lamellar lattice constants			
DMSO / pH	6	7	10
0wt%	5.895	10.081	7.311
10wt%	6.003	6.196/ 8.933	
20wt%	5.821	5.865	6.438/ 9.801
33wt%	5.772	6.066	6.511/ 10.045

Table 4. **Lattice constants** and **structures** of **δ90** with various **DMSO** contents. **Blue H_2, greenish mixtures of H_2 and Pn3m, green Pn3m** and **red lamellar**.

From 0wt% to 10wt% the lattice parameter increased for the hexagonal structure but for higher DMSO contents it decreased. The lattice parameters of our samples were rather de-

creasing but this is opposed to the results of a Japanese research group, which found increasing lattice constants through the addition of DMSO. [42] Similar results to ours were found by L. de Campo. [43] It seems that the errors of our DMSO addition experiments were quite large what is reflected in the fluctuating values.

4.2.3.2.6. Floating bulk phases with different oleic acid/ tetradecane mixtures

Oleic acid is responsible for the structural change through its different space demand in the protonated and deprotonated state. We wanted to know how far the oleic acid could be replaced by tetradecane and the gel is still able to perform the phase transition. δ90 was used and the oleic acid in there was replaced up to 80wt% by tetradecane.
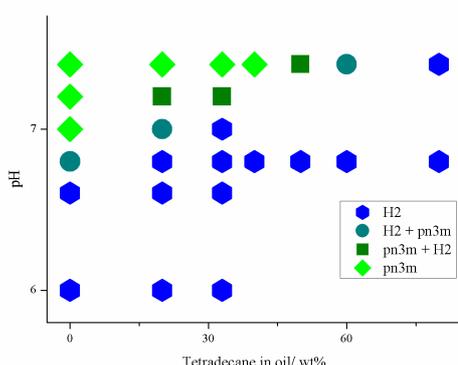
Figure 52:**δ90 phase diagram** with increasing content of **tetradecane** against the **pH**-value. Higher tetradecane amount than 40wt% does not lead to the phase conversion.

Through the addition of tetradecane the transition point shifted to slightly higher pH-values. While the conversion occurred without tetradecane at pH ~7, it took place for 20wt% at pH ~7.2.

When the tetradecane content was increased to over 40wt% of the oleic acid no pure Pn3m was recorded. The sample with 80wt% tetradecane was not showing any cubic signal.

The same experiment was performed with samples containing 10wt% PGE or 10wt% DMSO. For these experiments the tetradecane amount was 33wt%. The results out of these series were the same as for those without tetradecane. For the analysed range of tetradecane the influence of the other additives was dominant. The PGE containing samples changed to the cubic phase already at lower pH-values and the DMSO containing samples at higher values.

Samples with 10wt% PGE or 10wt% DMSO and 33wt% tetradecane of the oleic acid content behave the same as tetradecane free samples. 33wt% tetradecane have just a minor influence.

4.2.3.3. Polarisation microscopy with different oleic acid/ tetradecane mixtures

Additionally to the SAXS measurements we analysed the δ90 samples made from Dimodan U/J®, oleic acid and tetradecane with the polarisation microscope at an objective magnification of 20:1. With this method we were able to distinguish the hexagonal from other cubic phases. The H_2 structure is optical active and the twists the plane of polarised light. The microscope with crossed polarisers therefore records colourful pictures when H_2 is present and nothing when a cubic phase exists.
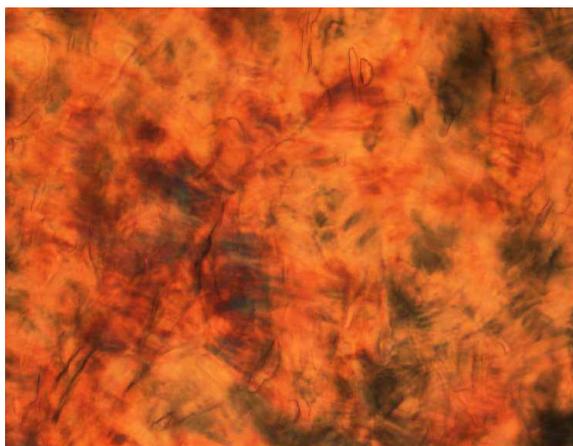
Figure 53: **δ90** with **5wt% oleic acid** and **5wt% tetradecane** at **pH 5.8**.
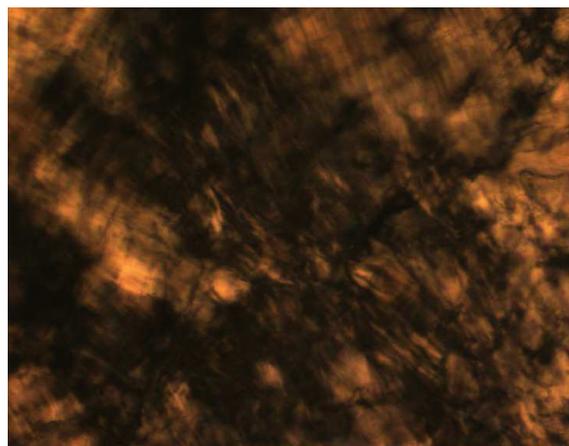
Figure 54: **δ90** with **5wt% oleic acid** and **5wt% tetradecane** at **pH 7.5**.

The two pictures above were taken from the same sample at different pH-values. The left one shows the probe at the starting point of pH 5.8 and the right one after increasing the pH. The typical colourful pattern disappeared more and more through the addition of NaOH for example the resulting structural transition occurred.
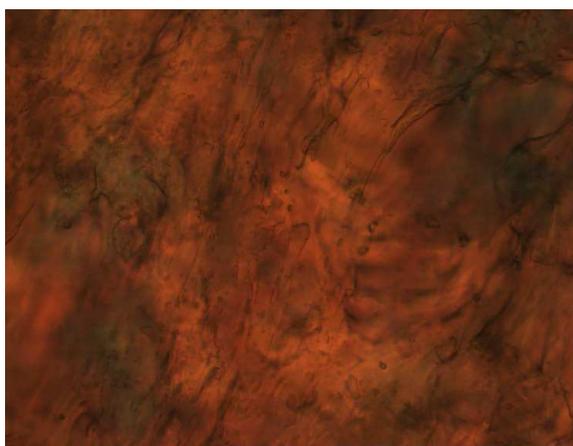
Figure 55: **δ90** with **2wt% oleic acid** and **8wt% tetradecane** at **pH 7.5**.

Figure 56: **δ90** with **6wt% oleic acid** and **4wt% Tetradecane** at **pH 7.5**.

The results of the examination with the polarisation microscope were matching with those from the SAXS measurements. The hexagonal structure was visible for all samples at lower pH-values. Higher pH-values led to the structural change and the colourful pictures disappeared. Samples with a mixed hexagonal and cubic structure were dark with colourful spots in-between.

The samples with a high amount of tetradecane did not change their structure through the addition of base. They remained hexagonal what was also observed with the polarisation microscope. Figure 56 displays the sample with 40wt% tetradecane of the oil content at pH 7.5. The picture is mainly black so we can assume that the dominating structure is cubic.

For mixed phases also the dominating structures were recorded. The more black spots, the higher the part of the cubic phase was. If we plot a phase diagram out of the microscopy data it would look similar to the SAXS phase diagram.

Polarisation microscopy is a suitable method for fast checks if a hexagonal phase is formed but SAXS remains the best choice for structure determination as we are not limited to hexagonal phases. SAXS enables us to calculate the lattice constants that give us further information about the structural dimensions.

4.2.3.4. Bulk phases with glutamine

According to the Hoffmeister series ions of different size have diverse properties. Therefore we examined the behaviour of glutamine compared to NaCl. Glutamine forms under acidic conditions mono cations and at neutral pH zwitterions. Also glutamine is bigger than NaCl. A future application of the responsive gels could be a drug delivering system and therefore glutamine was used as a cheap model additive, in order to study the influence to the structure and if the phase transition is somehow changed.
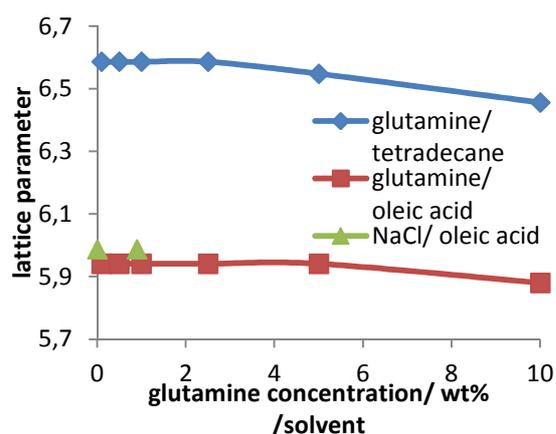
Figure 57: **δ90** containing various **glutamine** concentrations and the influence on the **lattice constant**.

The lattice constants of δ90 samples with tetradecane or oleic acid at different glutamine concentrations were determined. Therefore water saturated bulk phases with 50wt% water content were prepared. The aqueous solutions included 0.1wt% to 10wt% glutamine.

The obtained lattice parameters were constant at lower glutamine amounts. The lattice constants of samples containing tetradecane started to decrease after 2.5wt% glutamine, while oleic acid probes declined after 5wt%.

The oleic acid samples could be compared with measurements containing NaCl. The lattice constants are almost identical. As we experienced from the bulk phase release experiments the behaviour at low salt concentrations is the same while it changes at high concentrations.

Almost no differences between NaCl and glutamine were found at lower concentrations, therefore a glutamine concentration of 0.9wt% within the water was used for the pH depending measurements. The samples were prepared as floating samples in one case in a glutamine solution and in the other case a glutamine salt solution with 0.9wt% NaCl.

The samples without salt were not suitable, as the structural change through the pH increase was hardly observable. When salt was added we obtained good signals for hexagonal and cubic structures.
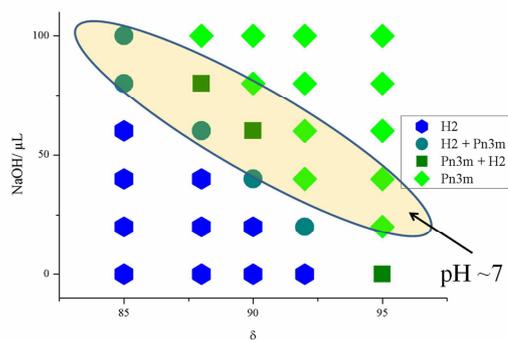
Figure 58: **Phase diagram** of **glutamine** and **NaCl** containing gels. very **simillar** behaviour compared to the **glutamine free** probes.

A phase diagram very similar to the samples just made from Dimodan U/J® and oleic acid was received. The diagram shows the same pH area of structural transition. Only at δ85 the development of the Pn3m was weaker and δ88 and δ92 converted to the Pn3m slightly earlier. δ90 and δ95 looked exactly the same as the samples without amine. The small differences for δ88 and δ92 are explained by minor inaccuracies of the preparation.

The addition of glutamine in a lower concentration was neither affecting the structural change nor the lattice constants. Therefore we can assume that a responsive gel loaded with lower quantities of glutamine like agents is behaving in the same manner as unloaded.

With the bulk phases floating in aqueous solutions we were able to observe pH induced structure changes. NaCl was a necessity. Without it only weak if any cubic signal were recorded. The physiological salinity of 0.9wt% was suitable.

Samples made from Dimodan U/J® and oleic acid had their structural transition around pH 7.4. The transition pH changed when additives like PGE or DMSO were used. PGE led to the Pn3m already at lower pH-values while DMSO shifted it to higher values. Depending on the DMSO or PGE amount the pH shifted. Only up to 20wt% PGE at a δ90 we were able to observe any hexagonal structure if the pH was decreased to pH 3. On the other hand if 20wt% or 33wt% of DMSO was added a cubic and hexagonal mixture was recorded when we went to pH 10.

We showed that we can substitute parts of the oleic acid by tetradecane. Replacing more than 50wt% of oleic acid by tetradecane is not suitable as the Pn3m development decreases with the tetradecane content and above this value the sample remains mostly hexagonal.

Adding glutamine did not affect the behaviour. At the analysed conditions, samples with glutamine showed the same behaviour as glutamine free probes. The system seemed to be tolerant against amines up to 5wt%.

4.3. Responsive bulk phase release experiments

Several gel compositions were found, which were able to change the structure through the pH variation. The structural transition was designed to start with the hexagonal phase and convert it to the bicontinuous cubic Pn3m. We have seen from the release experiments that a Pn3m loaded with a hydrophilic dye released the colorant to the excess water while the hexagonal restrained it. These facts made us built a diffusion cell, which should allow us to observe the migration of agents from one side to the other.

The diffusion cell consisted out of 3 divided chambers. The outer ones could be filled with different buffers. The chambers were separated through a middle chamber, which was used as a carrier for the bulk phase, fixed by a membrane.
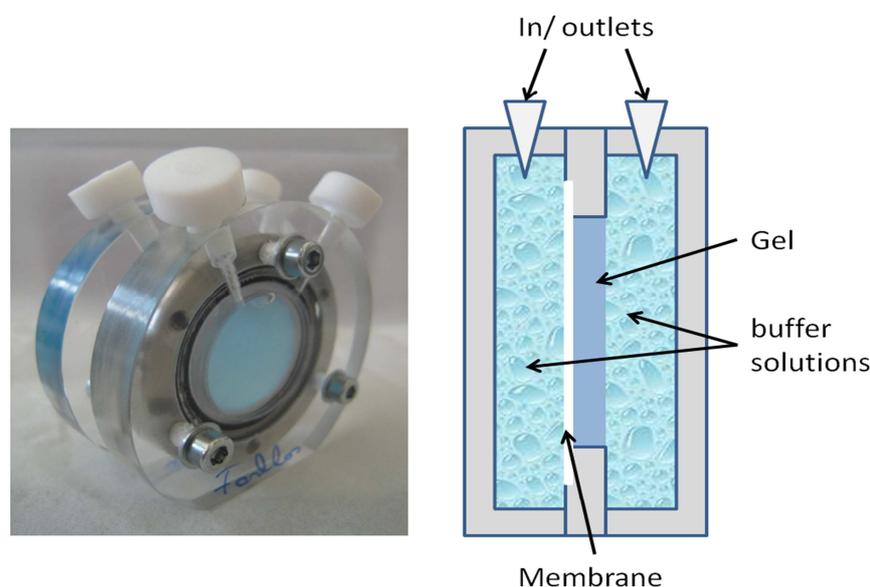
Figure 59: **Diffusion cell**. Picture and schematic drawing. 2 chambers separated by a membrane which carries the pH sensitive gel to observe a migration from one to the other chamber.

In a first set of experiments one chamber was loaded with a physiological phosphate buffer and Erioglaucine and the other chamber just with the buffer. δ90 with oleic acid was used as the bulk phase. Through the pH of the buffer the gel should transit to the bicontinuous Pn3m and we should observe in both chambers blue coloured solutions. This method was not suitable as the ratio of bulk phase to surrounding buffer and the buffer capacity was not sufficient, therefore a structural change was not observed.

The diffusion cell was substituted by a more basic setup. Photometer cuvettes were loaded with dyed δ90 bulk phases and different pH buffers were laid over. The structural change occurred and the dye was released. As the time needed to reach equilibrium is high this method had the advantage that experiments could be performed simultaneously, because several cuvettes were available.

More detailed studies of loading and releasing molecules from nanostructured bulk phases and dispersions can be found in the dissertation of Angela Chemelli [29] and the master thesis of Manuela Maurer. [41]

4.4. Responsive dispersions

Equilibration was one of the main problems of the bulk phases. Saturated bulk phases with high contents of PGE were time demanding in the preparation through centrifugation. Also afterwards, when the samples were homogenously prepared, the equilibration of pH-values afforded a lot of time. The floating bulk phases needed at least 24 hours to adapt to a new pH. Adding NaOH directly to the melted bulk phase was also not suitable as the fine-tuning and measurement of the pH-value was not possible. Therefore we moved to dispersions of our bulk phases prepared by ultrasonication or by shearing and addition of 7.5wt% F127 relative to the oil phase.

4.4.1. Sheared dispersions

As a start we prepared the dispersion of δ90 with oleic acid at a water to oil ratio of 2:1 and without salt. Several shearing temperatures were examined and the best working point was 90°C. At lower temperatures the bulk phase crystallised already in the shearing chamber and no sample was received.

A probe of the sheared δ90 was diluted 1:1000 with water and measured with the DLS. The data evaluation was performed with the preliminary ORT. The obtained particles had a hydrodynamic radius of 146.78nm ±0.79nm. In order to study the pH influence, NaOH was added to reach pH 7 after the dispersion process. The particle size was
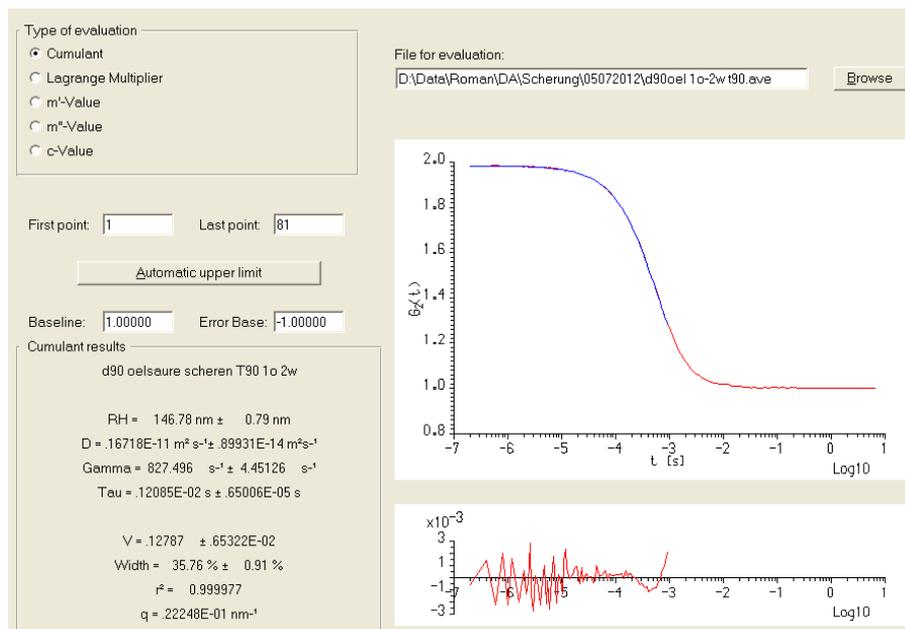
Figure 60: Screenshot of the **preliminary ORT** with the **hydrodynamic radius R_H** of δ90.

recorded as 227.87nm ±2.18nm.
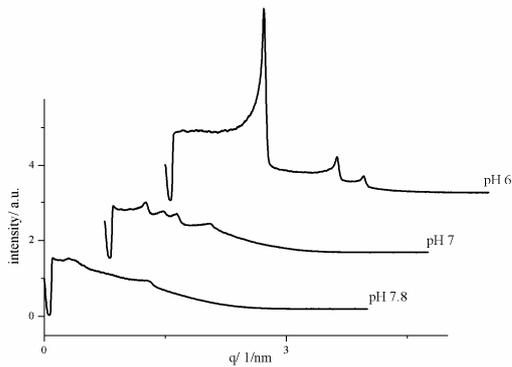
Figure 61: **Structures** of sheared **δ90** and the influence of different **pH**-values.

SAXS measurements showed that the dispersions were hexagonal at the starting point of pH ~6. At pH 7 we recorded a bad signal belonging probably to the Pn3m, when the pH was increased further we ended up in a loss of the signal. Through the addition of NaOH the dispersion became more and more gel like. It had a higher viscosity than at the beginning and it was challenging to measure the pH-value. The formation of vesicles is likely, as the observed changes are fitting to the behaviour of vesicles. The stabiliser F127 is supporting the formation of vesicles on the interface. Together with the behaviour of oleic acid that pushes towards a positive curvature only vesicles are plausible.

The structure of δ90 was recorded at the starting pH 6 and the increased pH-values pH 7 and pH 7.8. Additional temperature depending measurements were performed. The sample at pH 6 was in the temperature interval from 10°C to 60°C always hexagonal. At pH 7 we observed not a Pn3m but, through the temperature conditioning of the overnight measurement in the range of 10°C to 70°C, the Im3m was clearly visible. The signal of the Im3m increased with the temperature up to 60°C at this point also the H_2 started to develop. At 70°C Im3m and H_2 were both observed, with a minor signal of H_2.

The sample with pH 7.8 delivered no clear signal from 10°C to 37°C at 40°C an Im3m started to develop. In contrast to the bulk phases, the dispersion developed the Im3m.

As we experienced from the bulk phases the addition of salt results in better signals and structural transitions. A new δ90 was sheared with a 0.9wt% saline solution. We were not able to receive a dispersion. We got phase separated samples with pieces of bulk phase in an aqueous solution.

4.4.2. Ultrasonicated dispersions

Shearing was an excellent method to obtain higher amounts of one sample. As the shearing conditions were well controlled the produced dispersions were monodisperse. The disadvantage was the high temperature for the sample preparation. The shearing machine needed to be cleaned after every sample, because residuals were in there. This was time demanding as the machine had to cool down before it could be cleaned.

As we did not need huge amounts of one sample we went to ultrasonication. One probe was prepared within a few minutes and the cleaning was fast.

Samples with the same compositions as the bulk phase experiments were produced. There were probes containing just Dimodan U/J® and oleic acid at different δ-values, samples containing PGE, DMSO, glutamine, or various amounts of tetradecane. All of them were prepared with and without salt.

4.4.2.1. DLS measurements

Like the sheared dispersions also the ultrasonicated ones were characterised by the DLS. Each sample was measured at the starting pH of around pH 6 and an increased one at pH ~7. The amount of the stabiliser F127 was kept constant at 7.5wt% according to the oil content. We did not observe a composition or pH depending size distribution. The particle sizes were fluctuating widely. A mean particle size of 300nm ±100nm could be determined but the size distribution of each single sample was far more monodisperse and the standard deviation from the particle radius was just a few nm.

4.4.2.2. Titration of dispersions

Like acids and bases also the dispersions containing oleic acid could be titrated. The inflection point is indicating the pK_a and we were also expecting that the structural transition takes place at this pH, as there 50% of the acid is deprotonated.
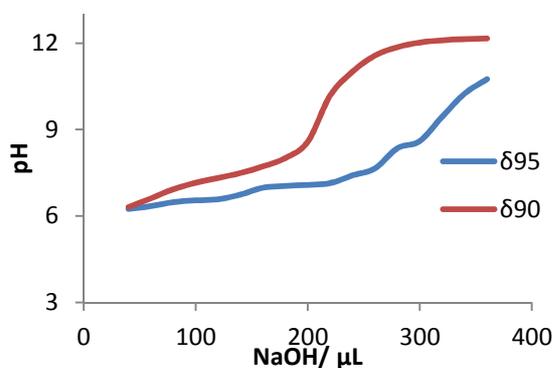
Figure 62: **Titration** curve of **δ90** and **δ95**. Slow equilibration and gel like intermediates at pH 7 made it difficult to measure.

The titration was performed twice manually and twice by auto titration for δ90 and δ95.

The results of the titration are of low quality and hard to reproduce. We estimated the pK_a around pH 8.

The main problem was the pH measurement when NaOH is added. The first steps were going quite well. It needed some time till the sample equilibrates (minutes to hours). Reaching the area around pH 7 made it even harder to obtain the value as the sample turned to a highly viscous liquid or even to solid gels. A further increase to pH 9 led again to a decrease of the viscosity.

Figure 63: Example of a **gel like dispersion** at **pH 7**.

The results from the auto titration were even worse. Better data were produced by Chemelli. She found the pK_a of 7.32 for the same system and mentioned the pK_a decrease through the addition of GMO. [29]

We found pK_a's depending on the sample between 8 and 9 and high viscous liquids/gels around pH 7 were observed. The "solid" gels were most likely formed out of vesicles, as they can enclose huge amounts of water. The sample in the picture consisted of a δ90 sample and contained 90wt% water.

4.4.2.3. SAXS results

Similar to the dispersions obtained from shearing, the SAXS signal of the ultrasonicated samples was quite bad. The dispersions were not diluted as they only contained 10wt% lipophilic phase and 90wt% water therefore the contrast was already low. The low oil content required an increased exposure time of 3 times 10 minutes.

4.4.2.3.1. Salt free samples

From the bulk phases we experienced that probes containing no salt develop the cubic structure worse than those with salt. The dispersions have different properties so they might build up the cubic phase better. We showed with the sheared dispersions that a structural transition was possible, but not great.
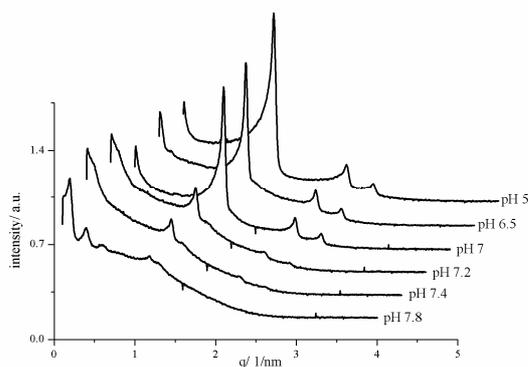
Figure 64: **δ90** dispersion at different **pH**-values. A **decrease** of the **hexagonal** phase through the increase of the pH-value was observed.
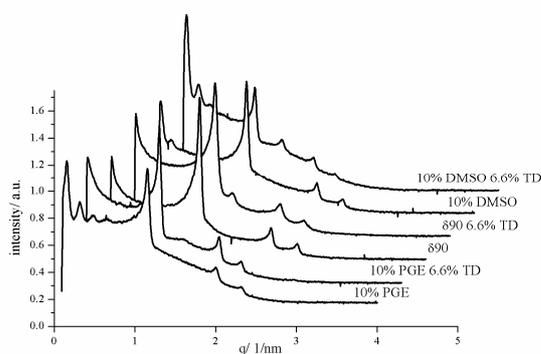
Figure 65: **Structures** of **δ90 dispersions** with different compositions at **pH 7**. Samples include PGE, DMSO as well as Tetradecane (TD).

Our standard reference sample like all the others too was spiked with NaOH to obtain various pH-values. In contrast to the sheared sample we were not observing a cubic phase around pH 7. Increasing the pH-value led to an decrease of the H_2 signal. At pH 7.2 the hexagonal peaks were already weak and at pH 7.8 no clear signal was observed.

For dispersion containing 10wt% PGE we expected a cubic structure even at lower pH-values and for those containing DMSO at higher values. Also the substitution of oleic acid with tetradecane should result in a higher amount of NaOH needed to perform the structural transition.

We were not able to record any of these expected properties as we were not able to obtain either the cubic Pn3m or the Im3m. Figure 65 compares the structure of δ90 samples with different additives at pH 7. All of them are hexagonal. The sample containing 10wt% DMSO and 6.6wt% tetradecane had an additional peak after the first H_2 peak which could not be identified. At higher pH-values we got for all of them scattering functions that indicated. The existence of vesicles around pH 7 was also very likely as this would explain the transition of the dispersions to solid gels.

4.4.2.3.2. Dispersions containing salt

The results from the dispersions were so far not satisfying. Therefore we made another attempt to create salt containing dispersions. When all the compounds, also containing salt, were mixed together and ultrasonicated we did not get dispersion. As soon as the ultrasonicator stopped the phases separated. The same happened with the shearing machine. When a salt free dispersion was prepared in a first step and salt was added in a second step we received stable dispersions.
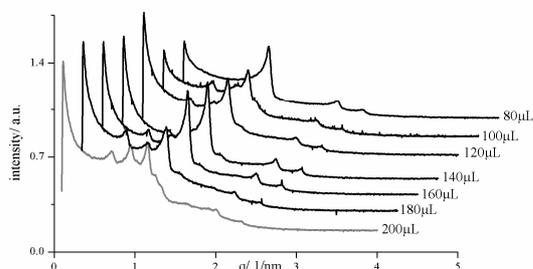
Figure 66: **δ90 dispersion** containing **salt** and different amounts of **NaOH.** Starting at the H_2. At **200μL NaOH** the cubic **Im3m** was observed.

With this preparation method we were able to record similar results as we got with the sheared samples. At higher amounts of added NaOH (200μL) we observed an Im3m phase. The 200μL NaOH were corresponding to a pH of 7.2.

Also the salt containing samples became more viscous at higher pH-values but they were not solid.

Differences of other compositions were not recorded as they have not been prepared except for glutamine containing dispersions. Those samples behaved the same way as the standard δ90.

Dispersions were useful as they equilibrated faster than the bulk phases, but it was difficult to observe any desired structural transition. The addition of salt helped at bulk phases but the dispersions were not stable unless the salt was added after the dispersion was prepared. Also the pH-value is difficult to set up as the samples become highly viscous or even gel like solid.

When cubic structures were recorded they were Im3m instead of Pn3m as in the bulk phases. The titration, although of low quality, confirmed the pH-value where the structural transition occurred.

5. Conclusion

The release experiments confirmed the expected behaviour that diffusion out of bicontinuous cubic phases is faster than out of enclosed phases such as the inverse hexagonal or the discontinues cubic Fd3m. [11] [13] [29] [41] [55] The Ia3d bulk phases showed a reduced release when they were exposed to high salt concentrations, because of a structural change towards the Fd3m occurred.

Water saturated and water unsaturated systems were observed as bulk phases. For the water unsaturated systems 20wt% of water content was suitable because no signals belonging to the surfactant crystals were found. Peak shifts were recorded through salt addition. The structures stayed the same but lattice parameters were increased, when salt was added (0.09wt% to 0.9wt% NaCl). [46] [54] Variation of the pH through NaOH addition resulted in cubic structures with broad signals. As the grade of water saturation was too low, the added amount of base was insufficient to transfer the hexagonal phase completely to the cubic phase.

Salt addition resulted in the same behaviour for plain water saturated phases as for the unsaturated ones. The pH dependency was clearly observed. Through the addition of base, the hexagonal phase transformed into cubic Pn3m and if the NaOH content was further increased we ended up with a lamellar phase. The lamellar phase is according to experiments that were performed with sodium oleate. [31] As we were working with the bulk phase the exact pH-value could not be controlled. A first pseudo binary phase diagram describes that phase transitions towards the Pn3m are easier obtained when the δ-value is higher. (Ideal δ89-δ92) By the substitution of 20wt% of the oleic acid with tetradecane and NaOH addition we determined a pure Pn3m phase.

To control the pH, water saturated bulk phases in excess water were prepared. With this method we were able to adjust the pH at suitable values. The equilibration of the bulk in excess water was the crucial point as a minimum of 24 hours was necessary. Equilibrations over 3 days were the best. Negrini and Mezzenga equilibrated their bulk phases in thin layers in a specially constructed diffusion cell. [55]

According to the temperature behaviour our cubic samples were stable over a wide range. At temperatures above 60°C we observe a transformation to hexagonal phases. [63]

Various compositions were analysed about their pH behaviour. The system based on Dimodan U/J®, water and oleic acid became cubic around pH 7. Through increased amounts of oleic acid also the amount of required base increased. The pH-value where the structural change occurred stayed the same.

PGE and DMSO had opposite effects. [42] PGE decreased the pH for the structural transfer, while DMSO increased it. PGE was pushing strong towards the cubic phase. With increased PGE content the cubic structure was developed even under very acidic conditions (pH ~3) and for lower δ-values (δ90). High PGE amounts are not suitable for a hexagonal to cubic transition as the hexagonal phase was not built at δ90 or above. An application that requires lower δ-values needs addition of PGE as it shifts the phase diagram to the left. [41]

DMSO based phases required on the other hand higher pH-values, as DMSO has the opposite effect on the curvature than the deprotonated oleic acid. More oleic acid needs to be deprotonated to compensate the effect of DMSO. Higher amounts of DMSO prefer the hexagonal phase and even under basic conditions the influence of the oleic acid was too weak to create the phase change. The transition pH was shifted up to pH 10 by the addition of DMSO.

Phases of different compositions with a δ-value of 90 showed the best results. In those phases up to 50wt% of oleic acid could be replaced by tetradecane. This range could be increased by the addition of PGE.

Other charged molecules like the zwitterions glutamine showed no effects. But all samples required a physiological salinity to obtain the cubic structures. This is according with the increased repulsion through the deprotonation of oleic acid. [46]

The bulk phases were tuned to ideally fit as a drug delivering material in the human body through the intestine. Systems under acidic conditions are hexagonal and therefore show low release of loaded molecules and through pH increase the cubic Pn3m is developed. Parameters to adopt the compartment sizes and pH ranges are given. [29] [55]

The dispersions on the other hand were not working well. Salt addition led to phase separation but a minimum salinity is needed to obtain the cubic structures. The phase separation can be avoided when the salt is added after the dispersion. Also the pH variation caused problems. Close to the pH where we expected the cubic phase the dispersion became highly viscous. Vesicles were formed, which is in accordance with the observation of Salentinig and Borné. [31] [53] The pKa determination under these conditions was roughly possibly and was around 7. Nevertheless also under these circumstances a cubic phase was obtained. The Im3m that we found is also fulfilling the requirements for drug delivering purposes as it is bicontinuous. The dispersions still need to be optimised but the δ-value of 90 seems to promising. Also the influence of F127 has to be checked, eventually by replacing it by nanoparticles (Pickering emulsions).

6. References

1. **Seddon, J. M.** Structure of the inverted hexagonal (HII) phase, and non-lamellar phase transitions of lipids. *Biochim Biophys. Acta.* 1031, 1990, pp. 1-69.

2. **Briggs, J., Chung, H. and M., Caffrey.** The Temperature-Composition Phase Diagram and Mesophase Structure Characterization of the Monoolein/Water System. *J. Phys II France.* 1996, Vol. 6, pp. 723-751.

3. **Qui, H. and Caffrey, M.** The phase diagram of the monoolein/water system: metastability and equilibrium aspects. Biomaterials. *Biomaterials.* 2000, Vol. 21, pp. 223-234.

4. **de Campo, L., et al.** Reversible Phase Transitions in Emulsified Nanostructured Lipid systems. *Langmuir.* 2004, Vol. 20, pp. 5254-5261.

5. **Demus, D., et al.** *3 High molecular weight liquid crystals.* s.l. : Wiley-VCH, 1998. pp. 342-353.

6. **Myers, D.** *Surfaces, Interaces, and Colloids: Principles and Applications.* 2. New York [i.a] : Wiley-VCH, 1999.

7. **Hyde, S. T.** Bicontinuous structures in lyotropic lipids in liquid crystals and crystalline hyperbolic surfaces. *Current Opinion in Solid State & Material Science.* 1996, Vol. 1, pp. 653-662.

8. **Seddon, J. M.** Surfactant liquid crystals. *Current Opinion in Colloid Interface science.* 2001, pp. 242-243.

9. **Luzzati, V., et al.** Cubic phases of lipid-containing systems. Elements of a theory and biological connotations. *J. Mol. Biol.* 1993, Vol. 229, pp. 540-551.

10. **Glatter, O.** Physical Chemistry I - Structure and Matter. University Graz : CHE.317, lecture WS 2009.

11. **Hyde, S. T., et al.** A cubic structure consisting of a lipid bilayer forming an infinte periodic minimum surface of the gyriod type in the glycerolmonooleate-water system. *Zeitschrift fuer Kristallographie.* 1984, Vol. 168, 1-4, pp. 213-219.

12. **Kaasgaard, T. and Drummond, C. J.** Ordered 2-D and 3-D nanostructured amphiphile self-assembly materials stable in excess solvent. *Phys. Chem. Chem. Phys.* 2006, 8, pp. 4957-4975.

13. **Boyd, B. J., Dong, Y.-D. and Rades, T.** Nonlamellar liquid crystalline nanostructured particles: advances in materials and structure dtermination. *Journal of Liposome Research.* 2009, Vol. 19, 1, pp. 12-28.

14. **Salonen, A., Muller, F. and Glatter, O.** Dispersions of Internally Liquid Crystalline Systems Stabilized by Charged Dislike Particles as Pickering Emulsions: Basic Properties and Time-Resolved Behavior. *Langmuir.* 2008, Vol. 24, pp. 5306-5314.

15. **Guillot, S., et al.** Direct and Indirect Thermal Transitions from Hexosomes to Emulsified Micro-Emulsions in Oil-Loaded Monoglyceride-Based Particles. *Coll. Surf.* 2006, 291, pp. 78-84.

16. **Salonen, A., Guillot, S. and Glatter, O.** Determination of Water Content in Internally Self-Assembled Monoglyceride-Based Dispersions from the Bulk-Phase. *Langmuir.* 2007, 23, pp. 9151-9154.

17. **Israelachvili, J. N., Mitchel, D. J. and Ninham, B. W.** Theory of self-assembly of hydrocarbon amphiphiles into micelles and bilayers. *Chem. Soc. Faraday Trans.* 1976, 2(72), p. 1525.

18. **Mitchell, D. J. and Ninham, B. W.** Micelles, vesicles, and microemulsions. *Journal of the Chemical Society, Faraday Transactions 2: Molecular and Chemical Physics.* 1981, Vol. 77, 4, pp. 601-629.

19. **Isrealachvili, J. N. and Degiorgio, V.** *Physics of Amphiphiles: Micelles, Vesicles and Microemulsions.* Amsterdam : North-Holland Physics Publishing:, 1985.

20. **Sjolund, M., Rilfors, L. and Lindbolm, G.** Reversed Hexagonal Phase Formation in Lecithin Alkane Water-Systems with different Acyl Chain Unsaturation and Alkane Length. *Biochemistry.* 1989, Vol. 28(3), pp. 1323-1329.

21. **Sagalowicz, L., et al.** Monoglyceride self-assembly structures as delivery vehicles. *Trends in Food Science & Technology.* 2006, Vol. 17 (5), pp. 204-214.

22. **Templer, R. H., Khoo, B. J. and Seddon, J. M.** Gaussian curvature modulus of an amphiphilic monolayer. *Langmuir.* 1998, Vol. 14 (21), pp. 7427-7434.

23. **Bragg, W. L. and Thomson, J. J.** The diffraction of short electromagnetic waves by a crystal. *Proceedings of the Cambridge Philosophical Society.* 1914, 17, pp. 43-57.

24. **Yaghmur, A., et al.** Oil-Loaded Monolinoelein-Based Particles with Confined Inverse Discontinuous Cubic Structure (Fd3m). *Langmuir.* 2005, 22, pp. 517-521.

25. **Angelov, B., et al.** SAXS investigation of a cubic to a sponge (L3) phase transition in self-assembled lipid nanocarriers. *Physical Chemistry Chemical Physics.* 2011, 13, pp. 3073-3081.

26. **Borg, R. J. and Dienes, G. J.** *The Physical Chemistry of Solids.* s.l. : Academic Press, 1992.

27. **Mezzenga, R., et al.** Shear rheology of lyotropic liquid crystals: A case study. *Langmuir.* 2005, Vol. 21 (8), pp. 3322-3333.

28. **Constantin, P., et al.** Connectivity of the Hexagonal, Cubic, and Isotropic Phases of the C12EO6/H2O Lyotropic Mixture Investigated by Tracer Diffusion and X-ray Scattering. *J. Phys. Chem. B.* 2001, 105, pp. 668-673.

29. **Chemelli, A.** *Optimized Loading and Sustained Release in Nanostructured Dispersions.* Karl-Franzens-University Graz : dissertation, 2012.

30. —. Loading and release in dispersions of internally self-assembled particles (Isasomes). Graz : Karl Franzens University, 2008.

31. **Borne, J., Nylander, T. and Khan, A.** Phase Behavior and Aggregate Formation for the Aqueous Monoolein System Mixed with Sodium Oleate and Oleic Acid. *Langmuir.* 2001, 17, pp. 7742-7751.

32. **Kirk-Othmer.** *Chemical Technology of Cosmetics.* s.l. : John Wiley & sons Inc., 2013.

33. **Barnes, I. S.** *Microstructure of Bicontinuous Phases in Surfactant Systems.* Australian National University : Dissertation, 1990.

34. **Amar-Yuli, D. and Garti, N.** Transistions induced by solubilized fat into reverse hexagonal mesophases. *Colloid Surface B.* 2005, 43 (2), pp. 72-82.

35. **Wu, D. G., et al.** Orientation and lateral mobility of insuluble Tempo amphiphiles at the water/air surface. *Electrochimica Acta.* 2006, 51, pp. 2237-2246.

36. **Salentinig, S.** *Lipid Digestion.* Karl-Franzens-University Graz : Dissertation, 2010.

37. **Gruner, S. M.** Intrinsic Curvature Hypothesis for Biomembrane Lipid-Composition - a Role for Nonbilayer Lipids. *P. Natl. Acad Sci. USA.* 1985, 82 (11), pp. 3665-3669.

38. **Yeh, M. C., Chen, C. M. and Chen, L. J.** Effect of Amphiphile Hydrophobicity of wetting Behaviors of Ternary Water + Oil + Amphiphile Mixtures: A Density Functional Theory Approach. *J. Phys. Chem. B.* 2004, 108, pp. 7271-7279.

39. **Pitzalis, P., et al.** Characterization of the liquid-crystalline phases in the glycerol monooleate/diglycerol monooleate/water system. *Langmuir.* 2000, 16 (15), pp. 6358-6365.

40. **Yaghmur, A., et al.** Control of the internal structure of MLO-based isasomes by the addition of diglycerol monooleate and soybean phosphatidylcholine. *Langmuir.* 2006, 22 (24), pp. 9919-9927.

41. **M., Maurer.** *Lyotropic Liquid Crystals: Investigations on Loading and release of Hydrophilic Functional Molecules.* Karl-Franzens University Graz : Master thesis, 2012.

42. **Abe, S. and Takakashi, H.** A comparative study of the effects of dimethyl sulfoxide and glycerol on the bicontinous cubic structure of hydrated monoolein and its phase behavior. *Chemestry and Physics of Lipids.* 2007, 147, pp. 59-68.

43. **de Campo, L.** private correspondence. Canberra : s.n., 2012.

44. **Timasheff, S. N.** Controll of protein stability and reactions by weakly interacting cosolvents: the simplicity of the complicated. *Adv. Protein Chem.* 1998, 51, pp. 355-432.

45. **Collins, K. D. and Washabaugh, M. W.** The Hoffmeister effect and the behavior of water at interface. *Q. rev. Biophys.* 1985, 18, pp. 323-422.

46. **Takahashi, H., Matsuo, A. and Hatta, I.** Effects of chaotropic and kosmotropic solutes on the structure of lipid cubic phase: monoolein-water systems. *Mol. Cryst. Liq. Cryst.* 2000, 347, pp. 2318-238.

47. **Engelskirchen, S., Maurer, R. and Glatter, O.** Effect of glycerol addition on the internal structure and thermal stability of hexasomes prepared from phytantriol. *Colloids and Surfaces A: Physiochemical and Engineering Aspects.* 2011, 391, pp. 95-100.

48. **Rether, C., et al.** Self-association of an indole based guanidinium-carboxylate-zwitterion: formation of stable dimers in solution and the solid state. *Beilstein J. Org. Chem.* 2010, Vol. 6, 3.

49. **Ivanov, I. A., et al.** Mixed surfactant-polyzwitterion self-assemblies in aqueous solutions. *Colloids and Surfaces A: Physicochemical and Engineering Aspects.* 2006, 282, pp. 129-133.

50. **Estephan, Z. G., Jaber, J. A. and Schlenoff, J. B.** Zwitterion-Stabilized Silica Nanoparticles: Toward Nonstick Nano. *Langmuir.* 2010, 26 (22), pp. 16884-16889.

51. **Cistola, D. P., et al.** Ionization and Phase Behavior of Fatty Acids in Water: Application of the Gibbs Phase Rule. *Biochemistry.* 1988, 27, pp. 1881-1888.

52. **Nakano, M., et al.** Dispersions of Liquid Crystalline Phases of the Monoolein/Oleic Acid/Pluronic F127 System. *Langmuir.* 2002, 18 (24), pp. 9283-9288.

53. **Salentinig, S., Sagalowicz, L. and Glatter, O.** Self-Assembled Structures and pKa Value of Oleic Acid in Systems of Biological Relevance. *Langmuir.* 2010, Vol. 26 (14), pp. 11670-11679.

54. **Aota-Nakano, Y., Li, S. J. and Yamazaki, M.** Ejects of electrostatic interaction on the phase stability and structures of cubic phases of monoolein/oleic acid mixture membranes. *Biochmica et biophysica Acta.* 1461, pp. 96-102.

55. **Negrini, R. and Mezzenga, R.** pH-Responsive Lyotropic Liquid crystals for Controlled Drug Delivery. *Langmuir.* 2011, 57, pp. 5296-5303.

56. **Kalantzi, L., et al.** Characterization of the human upper gastrointestinal contents under conditions simulating bioavaliability/bioequivalence studies. *Pharmaceutical Research.* 2006, 23 (1), pp. 165-176.

57. **Fong, W.-K., Hanley, T. and Boyd, B. J.** Stimuli responsive liquid crystals provide 'ondemand' drug delivery in vitro and in vivo. *Journal of Controlled Release.* 2009, 135, pp. 218-226.

58. **Ericsson, B., Larsson, K. and Fontell, K.** A cubic protein-monoolein-water phase. *Biochimica et Biophysica Acta, Biomembranes.* 1983, 729 (1), pp. 23-27.

59. **Chemelli, A., et al.** Optimized Loading and Sustained Release of Hydrophilic Proteins from Internally Nanostructured Particles. *Langmuir.* 2012, 28, pp. 16788-16797.

60. **Boyd, B.** Characterisation of drug release from cubosomes using pressure ultrafiltration method. *International Journal of Pharmaceutics.* 2003, 260, pp. 239-247.

61. **Koppel, D. E.** Analysis of macromolecular polydispersity in intensity correlation spectroscopy: the method of cumulants. *J. Chem. Phys.* 1972, 57, pp. 4814-4820.

62. **Amar-Yuli, D. and Garti, N.** transitions induced by solubilized fat into reverse hexagonal mesophases. *Colloid Surface B.* 2005, Vol. 43 (2), pp. 72-82.

63. **Moitzi, C., et al.** Phase Reorganization in Self-Assembled Systems Through Interparticle Material Transfer. *Advanced Materials.* 2007, 19, pp. 1352-1358.

64. **Seddon, J. M., et al.** Inverse micellar phases of phospholipids and glycolipids. Invited Lecture. *Phys. Chem. Chem. Phys.* 2000, 2, pp. 4485-4493.

7. Appendix

7.1 Figures

7.2 Tables